AD-A055 675 SCIENCE APPLICATIONS INC MCLEAN VA F/G 17/1
ACOUSTIC FLUCTUATION MODELING AND SYSTEM PERFORMANCE ESTIMATION--ETC(U)
JAN 78 R C CAVANAGH N00014-76-C-0753
UNCLASSIFIED SAT-79-737-WA-VOL-1 NL

1 OF 2
ADA
055675

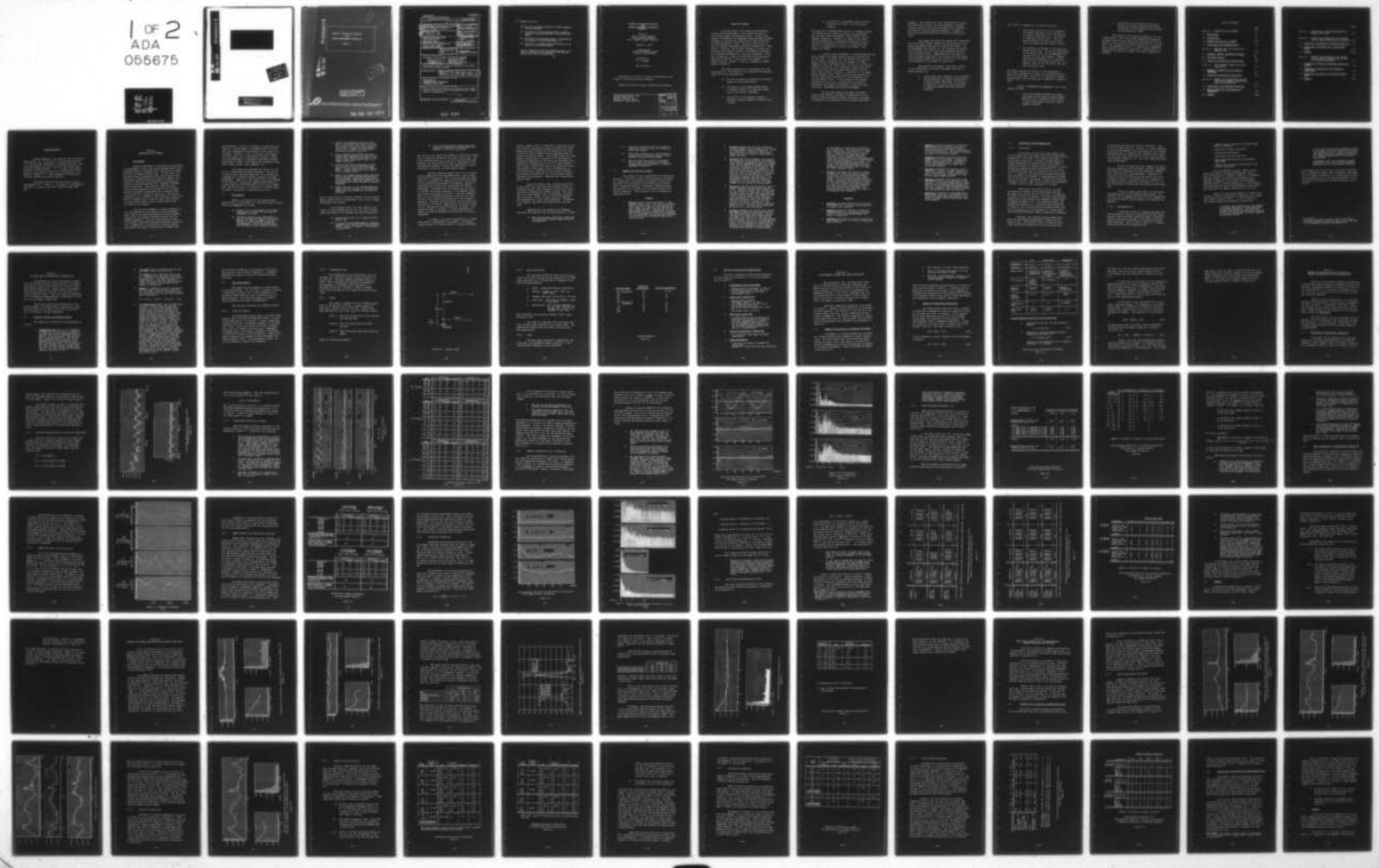

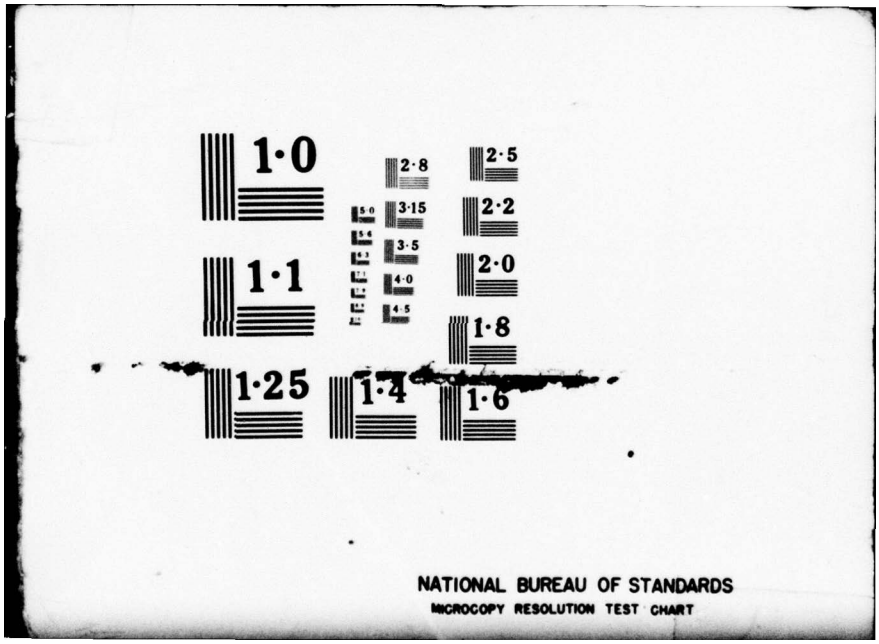
1·0
1·1
1·25
2·8
3·15
3·5
4·0
4·5
5·0
2·5
2·2
2·0
1·8
1·4
1·6
NATIONAL BUREAU OF STANDARDS
MICROCOPY RESOLUTION TEST CHART

ACOUSTIC FLUCTUATION MODELING
AND
SYSTEM PERFORMANCE ESTIMATION

VOLUME I

SAI
ATLANTA • ANN ARBOR • BOSTON • CHICAGO • CLEVELAND • DENVER • HUNTSVILLE • LA JOLLA
LITTLE ROCK • LOS ANGELES • SAN FRANCISCO • SANTA BARBARA • TUSCON • WASHINGTON

UNCLASSIFIED

MIL-STD-847A
31 January 1973

SECURITY CLASSIFICATION OF THIS PAGE (When Data Entered)

REPORT DOCUMENTATION PAGE	READ INSTRUCTIONS BEFORE COMPLETING FORM
1. REPORT NUMBER	2. GOVT ACCESSION NO. 3. RECIPIENT'S CATALOG NUMBER
4. TITLE (and Subtitle) (6) ACOUSTIC FLUCTUATION MODELING AND SYSTEM PERFORMANCE ESTIMATION, VOLUME I.	5. TYPE OF REPORT & PERIOD COVERED (9) Final Rept.
7. AUTHOR(s) (10) R. C. Cavanagh	8. CONTRACT OR GRANT NUMBER(s) (15) N0014-76-C-0753
9. PERFORMING ORGANIZATION NAME AND ADDRESS Science Applications, Inc. 8400 Westpark Drive McLean, VA 22101	10. PROGRAM ELEMENT, PROJECT, TASK AREA & WORK UNIT NUMBERS 65152N R0145 NR274-266
11. CONTROLLING OFFICE NAME AND ADDRESS Naval Analysis Program (Code 431) Office of Naval Research Arlington, VA 22217	(11) 12. REPORT DATE 4 January 1978 13. NUMBER OF PAGES 107
14. MONITORING AGENCY NAME & ADDRESS (if different from Controlling Office) (12) 412 p.	15. SECURITY CLASS. (of this report) UNCLASSIFIED 15a. DECLASSIFICATION/DOWNGRADING SCHEDULE

16. DISTRIBUTION STATEMENT (of this Report)

Approved for Public Release; Distribution Unlimited

(16) R0145 (17) R0145

17. DISTRIBUTION STATEMENT (of the abstract entered in Block 20, if different from Report)

Reproduction in whole or in part is permitted for any purpose of the United States Government.

18. SUPPLEMENTARY NOTES (14) SAI-79-737-WA-VOL-I

19. KEY WORDS (Continue on reverse side if necessary and identify by block number)

SONAR DETECTION
UNDERWATER SOUND TRANSMISSION
UNDERWATER AMBIENT NOISE

20. ABSTRACT (Continue on reverse side if necessary and identify by block number)

This two volume report documents an investigation into several aspects of the validity of the random-process approach. Among the topics considered are:

→ next page

DD FORM 1 JAN 73 1473 EDITION OF 1 NOV 65 IS OBSOLETE

UNCLASSIFIED
SECURITY CLASSIFICATION OF THIS PAGE (When Data Entered)

408 404

slt

20. ABSTRACT (Continued)

(a) the basic statistical properties of acoustic signal and noise fluctuations;

(b) the ability of the random-process models to properly simulate the important properties of the acoustic variables;

(c) the ability of the stochastic models to accurately predict measures of system effectiveness; and

(d) the choice of a stochastic model and estimation of its inputs, for a particular scenario.

Volume I summarizes the modeling procedure and gives the results and conclusions of the comparison of the stochastic process results with the acoustic data.

ACOUSTIC FLUCTUATION MODELING AND SYSTEM PERFORMANCE ESTIMATION VOLUME I

Report to

Office of Naval Research
Naval Analysis Program
Attn: James G. Smith, Code 431

January 4, 1978

Final Report
Contract N00014-76-C-0753
Task No. (NR 274-266)

Prepared by:
R. C. Cavanagh

SAI 79-737-WA

Approved for public release; distribution unlimited.

SCIENCE APPLICATIONS, INC.
8400 Westpark Drive
McLean, Virginia 22101
Telephone: (703) 821-4300

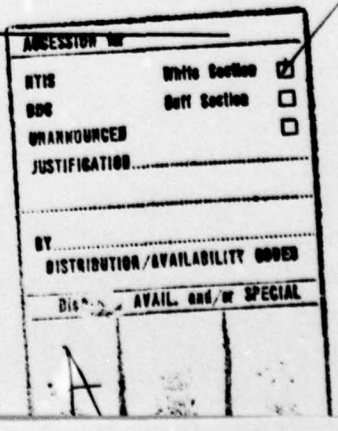

EXECUTIVE SUMMARY

A critical part of the analysis and estimation of sonar system performance is the characterization of the acoustic signal and background noise. Current techniques in performance and engagement modeling employ random-processes to simulate the long and short-term variations of these parameters in time. The usual justification is that the complex mechanisms governing the generation, transmission, reception, and processor response of signals and noise are sufficiently "random" to be modeled by stochastic processes determined by a few input parameters. Since such an approach is much more efficient than measuring or modeling the details of the acoustic environment, it is widely utilized. However, it has not undergone a comprehensive evaluation.

This report documents an investigation into several aspects of the validity of the random-process approach. Among the topics considered are:

(a) the basic statistical properties of acoustic signal and noise fluctuations

(b) the ability of the random-process models to properly simulate the important properties of the acoustic variables

(c) the ability of the stochastic models to accurately predict measures of system effectiveness

(d) the choice of a stochastic model and estimation of its inputs, for a particular scenario.

The ideal way to address these would be to compare stochastic simulations with measured acoustic and performance data for many ocean environments, sonar systems, and engagement geometries. However, the scope of this study and the availability of appropriate measurement data required the investigation to focus on a simplified test case for a representative acoustic environment, sonar system, and target.

A single ocean environment (in the Northeast Pacific during Summer) and target scenario has been selected for the test case. To ensure that the effects of the environmental acoustic parameters could be gauged, the study assumed a stable narrowband source (at 25 Hz), an idealized towed array receiver, and a processing system which automatically detects when the beam-output signal-to-noise ratio (SNR) exceeds a threshold. Evaluation of the random-process approach under these conditions then requires the detailed space/time properties of the transmission loss (TL) and ambient noise. A novel aspect of the present investigation is the use of state-of-the-art acoustic propagation and ambient-noise models to fabricate such a controlled, representative acoustic environment.

For the test scenario and target conditions, there is good reason to attribute fluctuations in TL to relative receiver movement through the source's multipath interference field (assuming little influence from ocean

dynamics). The acoustic TL "data" were generated from models which fully account for this mechanism. Similarly, a special ambient noise model was developed to simulate the dominant noise fluctuation mechanism: movement of many contributing surface ships through the interference field.

Once signal and noise time series were constructed with the acoustic models, several of the more popular random-process models were used to simulate the series. Input parameters (the trend in TL, the variance and decorrelation scales of TL and noise) were determined directly from the acoustic data. Comparisons were then made of the statistical properties of the acoustically and stochastically modeled signal and noise, as well as of the detection properties of the signal-to-noise ratio.

The principal conclusion of the study, subject to the limitations in the test environment and data, is stated generally as:

- Given proper input parameters, the stochastic-process approach can produce adequate simulations of signal and noise. The accuracy is sufficient to provide useful estimates of detection probabilities and detection histories.

This result is tempered by the observations that:

- The accuracy and utility of the approach are greatly dependent on the availability of accurate input data (e.g., the variance of beam-noise fluctuations). Such data may be difficult to obtain, and without them the predictions will usually be poor.

- The accuracy also depends on the particular random process used. This study concentrated on the popular ones, and the agreement with acoustic data was just adequate. However, significant improvements can be realized when the basic statistical properties (e.g., marginal density) are tailored to the variable and case at hand.

The report presents the details of the comparisons on which these judgements are based, and discusses the estimation of input data, the choice of a particular random-process model, and the prediction of measures of effectiveness.

Finally, recommendations suggested by the investigation include

- use of the computer packages and insight developed for the study to analyze measurement data and to extrapolate the results to other environments, receivers, and engagement scenarios.

- application of the theory and analytical models for multipath-induced fluctuations and ambient noise to generate better random-process models and inputs.

The details of the study are presented in a two-volume report. This first volume summarizes the modeling procedure and gives the results and conclusions of the comparison of the stochastic process results with the acoustic data. The companion volume is a compilation of appendices which provide references, calculations, documentation and background information to support the results reported in Volume I.

TABLE OF CONTENTS

ACKNOWLEDGEMENTS

Several members of the technical staff of Science Applications, Inc. contributed to the work reported here. C. W. Spofford was instrumental in defining the study, and provided insights and results for both the acoustic and stochastic modeling efforts. R. G. Stieglitz was responsible for the coding and execution of the majority of the computer packages; H. M. Garon designed and constructed the basic statistical analysis routines.

The study benefitted from the critical review and guidance of J. G. Smith, J. R. Simpson, T. Jayachandran, and CDR R. E. James of the Naval Analysis Program (ONR 431).

Section 1
INTRODUCTION AND SUMMARY

1.1 The Problem

Present techniques for predicting and evaluating the performance of Navy sonar systems depend heavily upon stochastic models to generate basic time series of signal and noise or signal-to-noise ratio. In particular, the deviation from a deterministic mean value is most often treated as a random process with specific temporal (e.g., stationary, Markovian with exponential autocorrelation function) and distributional (e.g., Gaussian, Rayleigh, Rician) properties. Time series of signal-to-noise ratio are thus generated as realizations of the random process and passed through detectors to simulate detection histories for individual encounters. Statistical accumulation over a number of such encounters yields estimates of probabilities of detection and other measures of system effectiveness, such as "mean holding time" and "time to lost contact."

The critical assumption in such an approach is that those aspects of the signal-to-noise environment which control the detection process are being accurately simulated by the specific stochastic process with its assumed parameters. The usual justification is that the extremely complicated processes governing the generation, transmission, and reception of acoustic signals and noise in the ocean are sufficiently "random" to be

characterized in terms of a stochastic process which depends on a limited number of parameters and is for the most part independent of the details of the acoustic environment. Clearly, if this is the case, such simulation techniques offer a considerable savings in effort over the measurement or modeling of the entire acoustic environment in terms of the underlying transmission loss, noise, target signal, sonar response, etc.

This study then addresses the question of validity of the stochastic-process approach: its ability to simulate the important properties of the acoustic environment and to provide accurate estimates of system performance. Implicit in this question are such problems as the choice of a particular random-process model for a given scenario, the determination of its input parameters, and the selection of a technique to actually generate sample time series of signal-to-noise ratio.

1.2 The Approach

Ideally, the validity of the random-process approach might be determined for a particular type of sonar system and engagement as follows.

(a) Select a set of environments which spans conditions of interest for the type of engagement and sonar.

(b) Carefully execute at-sea experiments to measure the detailed signal and noise properties for each environment, and for a variety of source/receiver geometries and movements. Use a controlled source and the selected sonar system as receiver.

(c) Subject the beamformer outputs to the sonar's processing and detection systems. The collected data would then consist of time series of signal and noise and detection for a variety of environmental and source/receiver conditions.

(d) Select random-process models and associated input parameters to simulate fluctuation and detection properties for the signal, noise, and detector input (e.g., signal-plus-noise).

(e) Generate statistical properties of signal and noise with the random-process models for the conditions of the experiments. Compare these simulation results with the measured data.

(f) Subject the random-process signal and noise data to the sonar's processing and detector algorithms. Compare the resulting detection histories and other measures of effectiveness with those observed in the measurements.

(g) Judge "validity" of the random-process approach from the accuracy of the simulated signal and noise properties and detection histories.

Each of these steps is certainly feasible, but the experimental effort would be overwhelming, even if only a single environment were treated.

In the present study, the seven steps are followed, but with alternatives for (a), (b), and (c) which allow the problem to be attacked with limited resources:

(ã) Perform the analsis for a single environmental case.

(b̃) In place of at-sea measurements, construct representative acoustic data with acoustic models. Limit the number of source/receiver geometries.

(c̃) Use an idealized sonar system, with time-invariant, deterministic beamforming, processing, and detector algorithms.

The choice of (ã) limits the ensemble of conditions treated here, a constraint imposed by the scope of the study. Use of an idealized sonar in (c̃) not only simplifies the data analysis, but also allows the study to concentrate on the environmental acoustic fluctuations unperturbed by uncertainties or variations in sonar-system behavior.

The most important substitution ($\tilde{b}$) is of acoustically modeled data for measurement data. Cost savings alone make it attractive. But it also provides the opportunity to investigate the sensitivity of the fluctuations to the underlying environmental and geometric factors by isolating each influence and identifying the dominant mechanisms. Confidence that the modeled data are realistic follows from recent advances in low-frequency propagation and noise modeling in which it has been suggested that not only averaged transmission loss (TL) and noise, but also their fluctuation properties can be accurately predicted. Modelable characteristics include overall distributions of intensity, range spectra and arrival angles for TL, time spectra and directionality for noise. This capability makes it feasible to create representative signal and noise environments with realistic fluctuation properties.

In summary, this study concentrated on a single North Pacific oceanographic environment, a few source tracks relative to a fixed receiver, a stable narrowband

source, a generic type of towed array system and an automatic detector operating on signal-to-noise ratio (SNR). Signal and noise time series were generated with state-of-the-art acoustic models for the idealized sonar response function and target. The acoustic model for transmission includes what is believed to be the important fluctuation mechanism for the test case (multipath interference for a moving source, but for a static medium). The automatic detector and statistical analysis routines were applied to the signal, noise, and SNR series to yield statistical properties of the acoustic variables and detection histories for the various target tracks and sonar characteristics. These are the "acoustically modeled" data.

Given the acoustic data, selected statistics of the signal and noise time series served as input to stochastic models, which simulate fluctuations by treating them as parameterized random processes. The focus was on the Gauss-Markov, Jump, and Ehrenfest processes, each of current interest in Navy operations analysis and determined by at most three parameters. "Stochastically modeled" data were thus generated for the test case.

Comparisons of the acoustic and stochastic data were then made with the following questions in mind:

(i) What are the basic statistical properties of acoustically modeled signal and noise fluctuations?

(ii) Under what conditions can the stochastic simulations properly model the signal and noise time series?

(iii) Under what conditions can the stochastic-process models accurately predict typical measures of system effectiveness?

(iv) How can predictive acoustic modeling be used to aid in the selection of random-process models and parameters for specific engagement scenarios?

1.3 Summary and Outline of Report

The results of this investigation are reported in two parts. This first volume briefly discusses the models, but concentrates on presenting the numerical results and analyses of the acoustically and stochastically modeled data. Background material, references, computer program descriptions, etc. are given in the second volume in the form of appendices. The contents of the two volumes are summarized below.

Volume I

- Section 2 gives a brief description of the acoustic models used in the study to generate signal and noise data, and then defines the test scenario in terms of the ocean environment, target geometry, receiver and source characteristics, etc. Idealization of source and receiver properties allows the investigation to concentrate on fluctuations attributed to a source moving through multipath interference fields.

- Section 3 summarizes the basic properties of the stochastic process models to be tested: the Gauss-Markov, Jump, and Ehrenfest. It also describes the method in which these models are used to simulate fluctuations in signal and noise.

- Section 4 derives and compares the statistical properties of acoustically and stochastically modeled transmission loss (TL) fluctuations, which themselves determine the signal and noise fluctuation characteristics. The properties investigated are limited to the first-order statistics, autocovariance, and selected level-crossing properties, all of which are found to be sensitive to the definition of the fluctuating part of the TL. The density function and spectrum of the acoustically modeled data are found to be consistent with the theory of multipath propagation, but are different from those assumed in the stochastic-process models.

- Section 5 considers the properties of acoustically modeled, omnidirectional ambient noise. The model assumes that surface ships are the sources of noise, and, for the test scenario, there are many ships contributing. As expected from theory, the omnidirectional noise is usually stable (small variance, large decorrelation times) and has density function consistent with that for many sources of multipath fluctuations. The exception is for the case that a single ship passes close to the receiver and dominates the noise for a long time period.

- Section 6 examines the acoustic and stochastic ambient-noise data as processed by the idealized horizontal towed array. Ten-hour time series of acoustically modeled noise are shown to be sensitive to the array's main-beam width, but not to sidelobe suppression if greater than 30 dB. As expected from theory, the noise density function becomes broader as the beamwidth is reduced and the variances are consistent with chi square variables whose degrees of freedom depend

on the number of ships which contribute to the fluctuations. The decorrelation times were large and not very sensitive to beamwidth. These properties of the acoustic data were found to be reasonably well-simulated by the stochastic processes - since the marginal densities often approached normal near the median and the autocovariance functions decayed smoothly and slowly. As far as level-crossing properties are concerned, the Jump process showed reasonable agreement with the acoustic data, at least for lower threshold values.

- Section 7 considers time series of signal-to-noise ratio (SNR) as generated from the acoustically and stochastically modeled signal and noise data for several target tracks. The level-crossing properties are directly associated with detection histories, so that the analysis concentrated on them. For the best stochastic-process simulation of signal and noise, given inputs derived from the acoustic data themselves, the detection-related properties were found to be reasonably well simulated.

Volume II

- Appendix A provides definitions of statistical properties for stochastic processes and fluctuation data analysis.

- Appendix B gives an overview of sonar performance prediction, including the various types of acoustic and system models and levels of simulation.

- Appendix C describes the acoustic signal and noise models used in the study, and discusses their validity.

- Appendix D surveys statistical fluctuation models based on an acoustic mechanism: varying multipath interference caused by source/receiver motion. The various statistical distributions and correlation functions are shown to be closely related.

- Appendix E describes and lists statistical properties of the stochastic fluctuation models tested in the study. Although not derived from properties of the acoustic field, these models are in common use in performance modeling.

- Appendix F discusses the approach used in the study to simulate a sonar signal processor and detector. Special attention is paid to the processor's integration times and the signal-excess detector.

- Appendix G provides justification for certain results used in the study about array response: the relative importance of transmission-loss and beam-pattern-induced fluctuations, conditions under which beam splitting can be ignored, and the effect of sidelobe suppression on noise fluctuations.

- Appendix H documents the algorithms used to model signal and noise, the numerical procedures for generating realizations of the random processes, and the statistical analysis package.

1.4 Conclusions and Recommendations

1.4.1 Conclusions

On the basis of the acoustically modeled data for the single test environment and limited target/receiver parameters of this study, the principal conclusion is: given proper input data, a stochastic-process model can produce simulations of signal-to-noise ratio (SNR) of sufficient accuracy to provide useful estimates of instantaneous and cumulative detection probabilities, as well as expected waiting times for detection and loss of contact. In addition, the random-process models considered here were found to be capable of simulating basic properties of the acoustic time series of signal and noise with reasonable accuracy, again given accurate input parameters. A careful review of these statements is in order.

First of all, the results are for one case, and cannot be extended without some further analysis. The implication is not that the study has to be repeated in detail for each new scenario, but rather that the basic properties of other acoustic environments and SNR's must be somehow estimated (e.g., with simplified models) and examined for amenability to stochastic-model simulation. In addition, only a few statistical properties were studied; extrapolation of the conclusions to include other detection-related measures cannot be made with confidence.

Secondly, the stochastic-process models were given the best possible opportunity to agree with the acoustic data: the detailed trend in TL and the calculated statistical properties of the TL and noise were

available and provided the inputs to the models. This is not the usual situation. In fact, if it were necessary to run acoustic models of the type used here or to collect measurement data to determine the stochastic model inputs for every new case, there would be little value in using the stochastic models at all: the "real" time-series data would be available.

Finally, although the basic temporal and distributional properties of the candidate stochastic processes were generally consistent with the acoustically modeled data, they were not in good agreement - especially in the tails of the distribution and the form of the autocovariance function. The effect may not be apparent in an overall review of detection statistics, for it is in the low probability events that such details become important.

In spite of these limitations, the conclusions encourage the use of the random-process approach. Included in the recommendations given below are suggestions for removing some of the shortcomings and improving the approach.

1.4.2 Recommendations

A substantial amount of computer machinery has been developed or applied in connection with this effort: acoustic noise and signal simulation models, statistical analysis and detector packages, and stochastic-process model algorithms. There is then a capability to examine other cases and other problems such as:

- higher acoustic frequencies and short-range tactical scenarios
- detection by fields of sonobuoys
- fixed system performance
- correlation for multiple arrays
- more complicated detectors and tracking algorithms
- higher order statistical properties of the acoustic parameters

Given the analysis routines, models, and insight into acoustic fluctuation mechanisms, there is also the opportunity to analyze, interpret, and simulate measured acoustic fluctuation and performance data. Although "validation" of the models is an extremely ambitious project, careful examination of a few selected data sets from well-controlled experiments would enhance the credibility of "model" studies such as this one.

There is a developing foundation of theory for multipath-induced fluctuations of signal and noise (Appendix D gives a partial survey). It can be applied to the present problem and extended in several ways:

- to provide input parameters for the stochastic-process approach via simplified models or analytical techniques for predicting acoustic fluctuation properties as functions of the ocean environment, encounter scenario, and receiver system.

- to rank order the scenario parameters according to their effect on fluctuations and detection properties, and to identify conditions for which source-motion-induced fluctuations will dominate those caused by the dynamic ocean medium

- to suggest alternative stochastic-process models with, e.g., more realistic marginal distributions or autocovariance functions

As an example for the last point, the results reported here in themselves suggest that an immediate improvement to the stochastic simulation of TL fluctuations for the test case would occur if the Jump process were to use a chi-square (or non-central chi-square) marginal distribution.*

*A stochastic process, derived from the GM process, with this marginal distribution has in fact been used in TL fluctuation analysis (see Appendix E).

Section 2
THE TEST CASE AND ACOUSTICALLY MODELED DATA

Transmission loss and noise predictions generated from state-of-the-art acoustic models for a special test scenario serve as the control data for this study. They provide deterministic, known acoustic environments which can be viewed as "real data" for the test of selected stochastic models. They also offer an explanation for the fluctuation mechanisms and an opportunity to improve the stochastic simulations.

This section gives brief descriptions of the acoustic models, the methods used to generate TL, signal and noise data for the specific test-case conditions, and the resulting test data themselves.

2.1 Acoustic, Source, and Receiver Models

The acoustically modeled data are generated as follows.

- Transmission loss (TL) is the fundamental variable and is predicted as a function of range with a model combining Parabolic Equation (PE) TL for waterborne paths and FACT TL for bottom bounce. The environment is assumed static, so that the primary mechanism for fluctuations is the movement of a source through the multipath interference field. For the environment and frequency (25 Hz) treated here, the model is fully capable of predicting the TL to the detail required (the range sampling period is 1/6 nm).

- The target moves at constant velocity and radiates a stable tone at 25 Hz.

- The receiver is an idealized towed array, at a fixed location and depth with a simple, deterministic response to plane waves (beam-pattern). Note that the use of stable source and receiver characteristics allows the study to concentrate on the acoustic fluctuations.

- Signal as a function of time is calculated for each target track directly from the TL, the target range $R(t)$ and bearing $\phi(t)$, the source level SL, and the array response $BP(\phi)$ according to

$$S(t) = SL(t) - TL(R(t)) + BP(\phi(t)). \quad (2\text{-}1)$$

- The ambient-noise model uses the same equation (2-1), but accounts for multiple sources. It uses a hypothesized set of surface ships, moving on straight-line courses across the basin and radiating noise correlated with their speeds. Ship source levels and courses are treated as random variables subject to constraints imposed by somewhat general bounds (e.g., speeds are 15 knots ±5 knots, courses are within 15° of 90° or 180°T). For each point in time, the radiated noise from each ship propagates to the receiving array. The resultant contributions are added incoherently (random phase), under the assumption that fluctuations associated with a coherent sum are typically averaged out by the signal processor's time integration. Transmission loss is derived from the model described above, but with a source depth of 60 feet and corrected to simulate loss from a near-surface source which radiates only away from the surface. The simulated noise time series is sampled every two minutes for the duration of a replication (e.g., 10 hours). Each replication is initialized by random selection of ships, speeds, courses and source levels.

More detailed information on the approach and acoustic model validity can be found in Appendix C. Appendix H describes the computer routines for generating signal and noise.

2.2 Test-Case Scenario

The single test environment is in deep waters of the North Pacific. Not only does it exhibit conditions of operational interest, but it also corresponds to a location at which data have been collected and the TL model evaluated. The ocean environment and surface-ship distributions are based on measurements.

The test-case conditions are summarized below.

2.2.1 Ocean Environment

The sound speed profile used to calculate transmission loss is derived from measurement data. It shows a thin mixed-layer at the surface, a classic thermocline, minimum at 3000 feet, and pressure gradient to the 14000 foot bottom. The bottom loss is also based on measurements, and is a constant 6 dB per bounce, independent of grazing angle. Wind speed is assumed to be moderate and thus has no effect on the calculations. These envionmental conditions are assumed to obtain throughout the 500-mile-radius "basin." The discussions on model validity of Appendix C support this assumption.

2.2.2 Transmission Loss

The transmission loss calculations to 500 nm are made for a 1000 foot receiver and for sources at 60 and 300 feet. The model assumes narrowband signals at 25 Hz. The TL estimates are completely deterministic and computed by the PE/FACT model mentioned in 2.1. Transmission loss as a function of range is sampled every 1/6 nm and used for both signal and noise fluctuations.

2.2.3 Target

The target is assumed to have a constant source level of 155 dB (μPa) at 25 Hz, a constant speed of 5 knots and a constant depth of 300 feet. Three tracks have been used for this study, each with constant course:

Track 1: Start 300 nm due north of the receiver and head due east

Track 2: Start 50 nm due north and travel due east

Track 3: Start 300 nm due north and travel due south

Figure 2-1 shows this geometry.

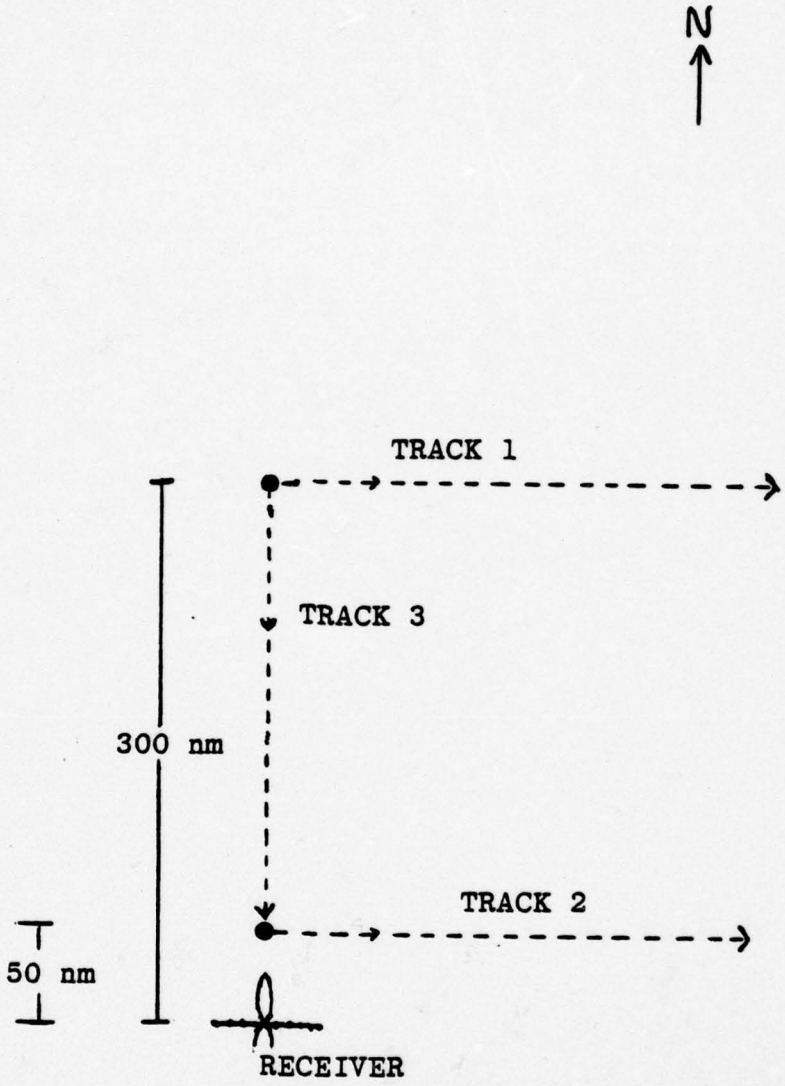

Figure 2-1. Target Tracks

2.2.4 Ship Distribution

The shipping distribution used in the calculations of the noise time series were generated by the DSBN model mentioned in 2.1 and described in Appendix H with the following parameters:

- speed: uniform distribution 10-20 knots
- bearing: uniform in $(75^{\circ}, 105^{\circ})$ and $(255^{\circ}, 285^{\circ})$
- average inter-ship arrival time: 0.78 hrs
- basin size: 1000 miles in diameter, array at the center
- source level: 161 + 60 log (speed/15) + 20 log [(160 + ℓ)/152] (dB re 1μPa, Hz), where ℓ is uniform in (-52, +52).

Once determined, each ship has constant course, speed, and source level.

This model is consistent with the traffic patterns and ship types observed in the scenario area. The expected ship density over the basin is one ship per 4500 square miles.

2.2.5 Array

The array model described in Appendices C and H was used, with parameters shown in Table 2-1. The omnidirectional response is also calculated.

Steering Angle	Beamwidth (half-power)	Sidelobe Suppression
90° (Broadside)	8°	30 dB
90°	8°	∞
90°	4°	30
90°	4°	∞
82° (8° east of broadside)	8°	30
74°	8°	30
65°	8°	30
56°	8°	30

Array Parameters

Table 2-1

2.3 The Set of Acoustically Modeled Data

The set of acoustically modeled data generated for this study with the models of 2.1 and the scenario of 2.2 consists of:

- **Transmission loss versus Range**
  - sampled every 1/6 nm from 0 to 500 nm
  - for receiver depth of 1000 feet and source depths of 60 and 300 feet.
  - at frequency 25 Hz
- **Signal Level versus Time**
  - sampled every 2 minutes
  - for target tracks 1, 2, and 3
  - for source depth of 300 feet and receiver depth at 1000 feet
  - for array response parameters of Table 2-1
  - for source level of 155 dB
- **Beam Noise versus Time**
  - 50 replications, each of duration 10 hours and one replication of duration 35 hours, sampled every 2 minutes
  - for ship parameters described in 2.2
  - for an omnidirectional receiver and for the array response parameters of Table 2-1 (simultaneous)
- **Signal-to-Noise-Ratio versus Time**
  - as constructed from Signal and Noise time series
- **Range-Averaged TL**
  - 2 nm and 5 nm intensity averages for above cases
  - A+BlogR fit (LMS) over 0-100 and 100-500 nm

Section 3
THE STOCHASTIC MODELS AND THEIR APPLICATION

The Gauss-Markov (GM), the Gauss-Jump (Jump), and to a limited extent the Ehrenfest random-process models have been selected for testing in this study, primarily because of their popularity in performance and engagement analyses. This section summarizes their basic properties as well as the manner in which they are used in this study to simulate fluctuations in signal, noise, and signal-to-noise ratio (SNR).

Additional supporting information can be found in Volume II. Appendix A gives definitions of stochastic-process properties. The rationale for the choice of the selected models and their specific properties are described in Appendix E. The computer algorithms for generating sample functions for these processes and the procedures for determining input parameters are documented in Appendix H.

3.1 Summary of Properties of Stochastic Processes

A stochastic (or random) process can be viewed as a random variable which depends on an index (usually time). The three models used in this study are mathematical in nature, with little basis in the physics of acoustic propagation and noise (although each is inspired by a physical phenomenon). Among the properties common to the three are:

- Each depends on at most three parameters.
- Each is stationary and ergodic (for the case that the mean is zero).
- Each has a one-dimensional (marginal) distribution which is Gaussian or approximately Gaussian.

Some of the distinguishing characteristics of interest in this study are listed in Table 3-1. Noteworthy are the sample-path structures (see Figure 4-5 for examples of continuous and jump paths) and the exponentially decaying autocovariance function which yields a smooth spectrum at low frequencies, with no dominant components.

3.2 Method for Simulating Fluctuations

The random-process models are used to simulate fluctuations of transmission loss with range and of signal and noise with time. In general, let $Z(t)$ denote one of these quantities and let $X(t)$ be the random-process model for simulating its fluctuations. The usual approach taken in engagement modeling is to treat the variable Z in decibel units, to predict its "deterministic" part $\overline{Z}(t)$, and then to simulate Z with

$$\hat{Z}(t) = \overline{Z}(t) + X(t). \qquad (3\text{-}3)$$

If $\overline{Z}$ is viewed as a "trend," chosen so that the residual fluctuation

$$Y(t) = Z(t) - \overline{Z}(t) \qquad (3\text{-}4)$$

	GM	Gauss-Jump	Ehrenfest
Parameters	μ,σ,λ	μ,σ,λ	n
Index Set	$t\varepsilon[0,T]$	$t\varepsilon[0,T]$	$k = 0,1,2,\ldots$
Sample Paths	continuous, nowhere differentiable	piece-wise constant, discontinuous at jumps	discrete (*paths constructed by* interpolation)
Joint Density	2-dimensional Gaussian	Not Gaussian	—
Marginal Density	Gaussian (μ,σ^2)	Gaussian (μ,σ^2)	Binomial (normalized)
Autocovariance Function	$\sigma^2 e^{-\lambda\|t\|}$	$\sigma^2 e^{-\lambda\|t\|}$	$(\frac{n-2}{n})^k$
Decorrelation Time	$1/\lambda$	$1/\lambda$	$-1/\ell n(\frac{n-2}{n})$
Power Spectrum	$\frac{2\sigma^2}{\omega^2+\lambda^2}$	$\frac{2\sigma^2}{\omega^2+\lambda^2}$	—

Level-Crossing Properties for the Gauss-Jump:

- Expected Waiting Time for Jump Process to Exceed L

$$= (1/\lambda)(1-P_D)/P_D \qquad (3\text{-}1)$$

- Probability that Jump Process Exceeds L Sometime in Interval [0,T]

$$= 1-(1-P_D)\exp(-P_D T/\lambda) \qquad (3\text{-}2)$$

where P_D is the probability that a Gaussian variable (μ,σ^2) *exceeds L.*

Some Properties of Stochastic Processes

Table 3-1

has mean zero, then the random-process model should have mean zero, and it will yield a good simulation $\hat{Z}$ of Z to the extent that the properties of X agree with those of Y.

In this study, the trend $\overline{Z}(t)$ of the acoustically modeled series Z(t) is found by averaging, and the residual fluctuation series Y(t) is analyzed by a statistical analysis package to determine its sample statistics (distribution function, moments, autocovariance function, etc.). These statistics of Y are in turn used as the inputs for the random-process model X.

In the case of noise time series, $\overline{Z}$ is a constant, long-term average. For transmission loss (TL(R)) versus range, the trend $\overline{TL}(R)$ is found as an intensity average over a range window (2 nm or 5 nm or the entire interval of interest). The simulated TL is then given by

$$\hat{TL}(R) = \overline{TL}(R) + X(R) \qquad (3\text{-}5)$$

The associated signal time series, before beamforming, is derived from the target's range R(t) and source level SL(t) as

$$\hat{S}(t) = SL(t) - [\overline{TL}(R(t)) + X(R(t))]. \qquad (3\text{-}6)$$

Finally, note that the stochastically modeled data are derived with the benefit of substantial information about the acoustic data - viz., the trend and the statistical properties of the fluctuations. In the usual

application, only the trend is predicted with any confidence (from data or acoustic models), so that the random-process parameters must be estimated from "experience." Hence, in this study, the stochastic models are given the best possible chance to generate accurate data.

Section 4

RESULTS FOR ACOUSTICALLY AND STOCHASTICALLY MODELED TRANSMISSION LOSS AND FLUCTUATIONS

This section derives and compares the properties of acoustically and stochastically modeled TL and its fluctuations. Considerable emphasis is placed on TL since in the stochastic data it is an essential component for signal, while for the acoustic data it drives both the signal and noise properties.

Among the topics covered here, one of the most important is the extraction of the "trend" or "deterministic part" of the TL. As discussed in Section 3, there are a number of ways in which this can be done, and the choice impacts heavily on the properties of the residual, which is then the fluctuation.

The first part of the section presents the properties of the TL fluctuations, and relates them to signal variations. In the second part, the ability of the stochastic-process models to simulate these properties is investigated.

4.1 Properties of Acoustically Modeled TL

The acoustic TL data generated for this study consist of a TL range series generated by the PE/FACT combination model, sampled every 1/6 nm from 0 to 500 nm, for a frequency of 25 Hz, a 1000 foot receiver, and two

source depths. The analysis here concentrates on the data for the deeper (300 foot) source depth, used to simulate the signal. Figure 4-1 is a plot of that function.

The number of cases (3 types of detrending over several range intervals) and scope of the study preclude the calculation of more than a few properties of the TL fluctuations. The ones chosen (see Appendix A) are those which determine stochastic-process inputs (mean, variance, decorrelation range), those which can be easily compared with basic stochastic-process properties (marginal distribution, autocovariance function), and those which relate to signal detectability (TL level-crossing statistics).

4.1.1 Fluctuation Properties as a Function of Smoothing

The usual prediction of mean TL can range from a simple curve to a detailed average over short ranges, and the resulting fluctuation properties can be very sensitive to the amount of smoothing. To investigate this, an average of the TL(R), called $\overline{TL}(R)$, was constructed using:

(i) an A+BlogR fit

(ii) a 5 nm intensity average

(iii) a 2 nm intensity average

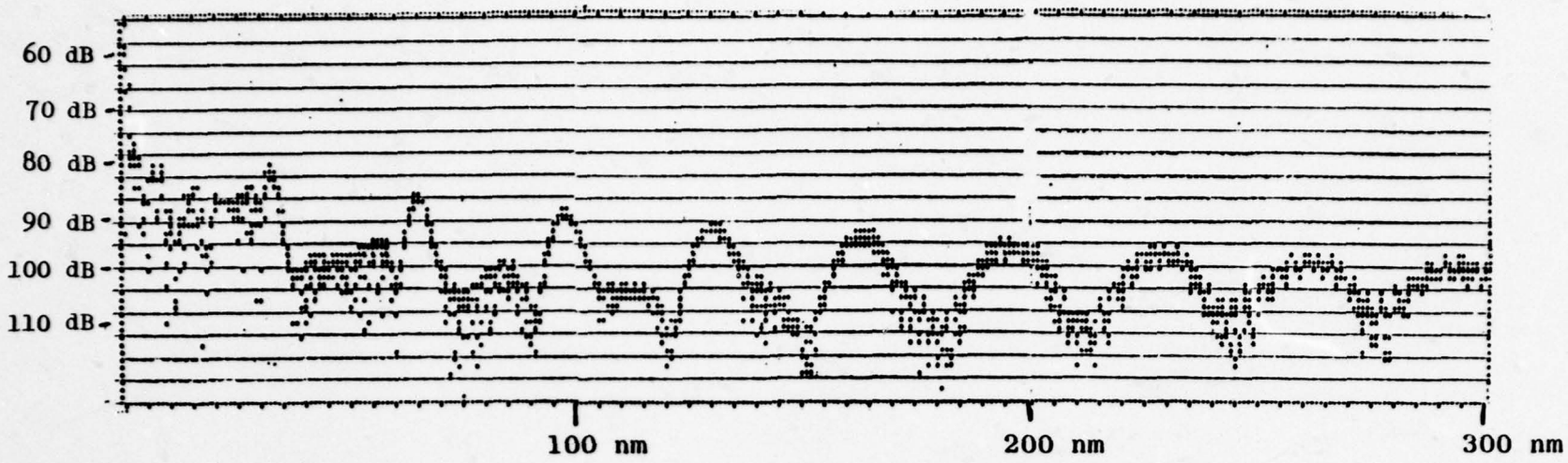

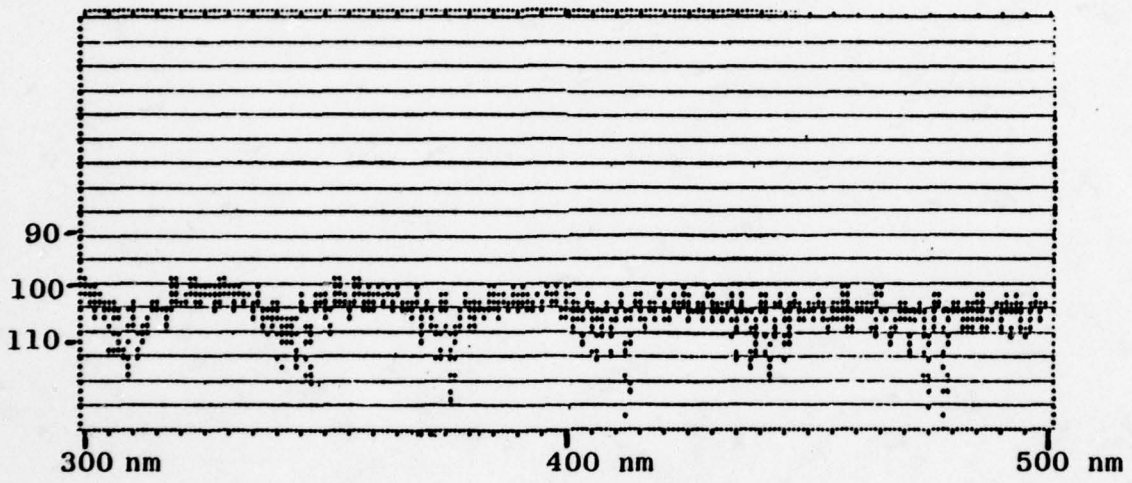

Acoustically Modeled TL for 300 Foot Source,
1000 Foot Receiver at 25 Hz

Figure 4-1

over various range segments. Then the "range fluctuation" was calculated for each case as

$$\Delta TL(R) = TL(R) - \overline{TL}(R).$$

For a source moving at rate R(t), it is $\Delta TL(R(t))$ which determines temporal multipath fluctuations and it is this term which the random-process models are intended to simulate. Figure 4-2 shows examples of $\Delta TL(R)$ for the three types of TL trends.

4.1.2 First-Order Statistics of $\Delta TL(R)$

The first-order statistical properties of the various versions of $\Delta TL(R)$ have been calculated and are summarized in Table 4-1. Notable are the following:

- The fluctuations corresponding to the detailed average $\overline{TL}$ (2 nm or 5 nm average) are extremely consistent from range-interval to range-interval beyond about 50 or 75 nm. This shows an absence of long-range trends (sometimes used as an indicator for stationarity). This is not the case for the short-range data, which have complicated regions of bottom-bounce propagation; nor is it true for the fluctuations about the A+BlogR average, which show convergence zones.
- In every case, the positive skewness means the ΔTL distributions are skewed to the right: the long tail to the right extends as far as 25 dB and corresponds to fades or "drop-outs" in the propagation, while the excursions below the mean are limited to about 5 dB.
- Note that the mean is not necessarily 0 when $\overline{TL}$ is an intensity average, and in fact is positive.

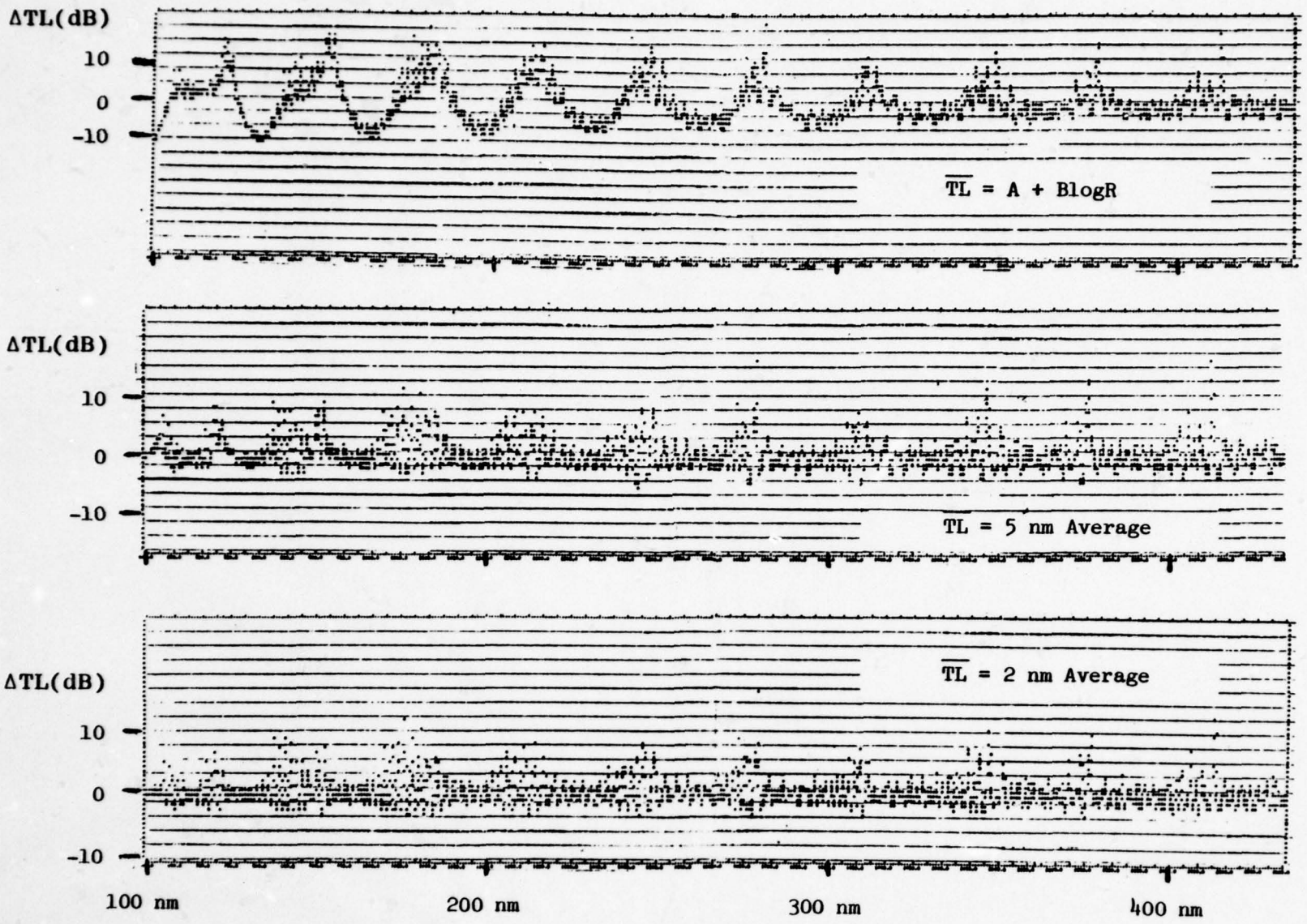

$\Delta TL = TL - \overline{TL}$

Fluctuation of TL with Range

Figure 4-2

$\overline{TL}$ = A+BlogR

Range Interval (nm)	Statistics (dB)				Percentiles (dB's)				
	μ	σ	skewness	kurtosis	0	20	50	80	100
100 - 200	.0	6.9	0.3	-.7	-11.4	-10.	-2	4	19.9
200 - 300	-.1	5.3	0.8	.0	- 7.7	- 6.	-4	2	21.0
300 - 400	-.3	3.5	1.4	2.2	- 5.7	- 5.7	-2	0	15.5
400 - 500	.4	3.2	1.9	5.7	- 4.8	- 4.	-2	0	18.0
100 - 300	.0	6.1	0.5	-.4	-11.4	- 8	-2	4	21.0
300 - 500	.1	3.4	1.6	3.7	- 5.7	- 4	-2	0	18.0
100 - 500	.0	5.0	0.7	0.8	-11.4	- 6	-2	2	21.0

5 nm Average

Range Interval (nm)	Statistics (dB)				Percentiles (dB's)				
	μ	σ	skewness	kurtosis	0	20	50	80	100
100 - 200	1.2	2.6	1.3	1.7	-2.9	-2	-2	0	12.7
200 - 300	0.8	2.6	1.4	3.8	-4.8	-4	-2	0	17.7
300 - 400	0.6	2.5	1.5	4.2	-4.6	-4	-2	0	14.5
400 - 500	0.8	3.1	1.8	5.6	-4.8	-4	-2	0	18.2
100 - 300	1.0	2.6	1.3	2.7	-4.8	-4	-2	0	17.7
300 - 500	0.7	2.8	1.7	5.5	-4.6	-4	-2	0	18.2
100 - 500	0.9	2.7	1.5	4.3	-4.8	-4	-2	0	18.2
2 - 12	5.1	6.2	.5	- .2	-4.8	-2	2	8	22.0
12 - 25	1.3	4.6	2.2	7.0	-5.1	-4	-2	4	23.8
2 - 25	3.1	5.7	1.2	1.2	-5.1	-4	0	6	23.8
2 - 74	2.5	5.0	1.4	2.6	-5.1	-4	0	4	26.0
75 - 150	1.3	2.9	1.3	2.0	-3.5	-2	-2	2	14.0
2 - 150	1.9	4.1	1.7	4.5	-5.1	-4	-2	2	26.0

2 nm Average

Range Interval (nm)	Statistics (dB)				Percentiles (dB's)				
	μ	σ	skewness	kurtosis	0	20	50	80	100
100 - 200	0.6	2.2	1.4	3.0	-3.5	-3.5	-2	0	12.4
200 - 300	0.6	2.2	1.6	5.4	-3.3	-3.3	-2	0	16.3
300 - 400	0.5	2.0	1.5	3.4	-3.1	-3.1	-2	0	10.6
400 - 500	0.7	2.4	2.4	8.6	-2.5	-2.5	-2	0	16.1
100 - 300	0.6	2.2	1.5	4.1	-3.5	-3.5	-2	0	16.3
300 - 500	0.6	2.2	2.1	7.7	-3.1	-3.1	-2	0	16.1
100 - 500	0.6	2.2	1.8	5.9	-3.5	-3.5	-2	0	16.3
2 - 12	2.8	5.5	1.2	1.1	-4.3	-4	-2	4	21.7
12 - 25	1.0	3.7	3.7	19.3	-3.5	-2	-2	0	23.8
2 - 25	1.9	4.7	2.0	5.0	-4.3	-4	-2	2	23.8
2 - 74	1.5	4.1	2.1	6.4	-4.3	-4	-2	2	25.0
75 - 150	0.6	2.4	1.5	3.1	-4.0	-2	-2	0	12.7
2 - 150	1.1	3.4	2.4	9.0	-4.3	-4	-2	0	25.0

Fluctuation Statistics for $\Delta TL = TL - \overline{TL}$

Table 4-1

Now in studying fluctuations of signal intensity, it is $-\Delta TL$ which is of interest. All of the statistics of Table 4-1 are applicable, with the following changes:

- The sign of the mean and skewness are changed indicating skewness to the left.
- The percentiles are reversed so that the long tails (up to 25 dB) are to the left and there are only small excursions (5 dB) above the mean.

The resulting properties are consistent with the theory (Appendix D) of intensity as a sum of randomly-phased multipath sinusoids. In fact, the various candidate intensity distributions (chi-square, noncentral chi-square, and log-normal) were transformed into dB's and tested against the sample distributions of $-\Delta TL$ over the 100-500 nm range interval. The results showed poor agreement for the log-normal, but very good agreement for the distributions predicted by theory for long-range, waterborne, multipath propagation (chi-square and non-central chi-square with 2 d.f.).

4.1.3 Temporal Properties of TL Fluctuations

The correspondence of range fluctuations in TL with temporal fluctuations of signal from a moving source has been emphasized throughout this report. In Appendix D some rationale for interpreting the spectral properties of the intensity in terms of the multipath propagation structure is presented. However, the scope of this study

has limited the investigation to one of the temporal properties of the TL (or signal) in dB's, as used in the stochastic models for signal fluctuations. In particular, the focus is on the autocovariance function form and the decorrelation time for the TL fluctuations.

Figure 4-3 shows an example of the normalized autocovariance functions for the TL fluctuations, for the three $\overline{TL}$ averages. As an aid to identifying the periodicities, the corresponding Fourier transforms have also been calculated and samples are shown in Figure 4-4. Important features derived from these and other cases include:

- The "decorrelation" ranges (to the 1/6 nm resolution available) are short in every case for fluctuations about the 2 nm and 5 nm averages - typically 1/3 to 1/2 nm. However, for the A+BlogR case, the first 1/e point occurs at 5 nm and the correlation can be high at great ranges.

- There is significant structure in the autocorrelation functions beyond the first zero-crossing, quite different from the exponential function assumed in the stochastic processes.

- The spectra for the three different averages ($\overline{TL}$) are nearly identical above a cutoff frequency corresponding to the averaging range. For the 100-500 nm range, notice important contributions at periods from about 1.5 to 4 nm and near 30 nm, with the last eliminated for the case of detailed averaging (2 or 5 nm), as expected. For the shorter range interval, there are peaks corresponding to periods in the neighborhood of 0.5 to

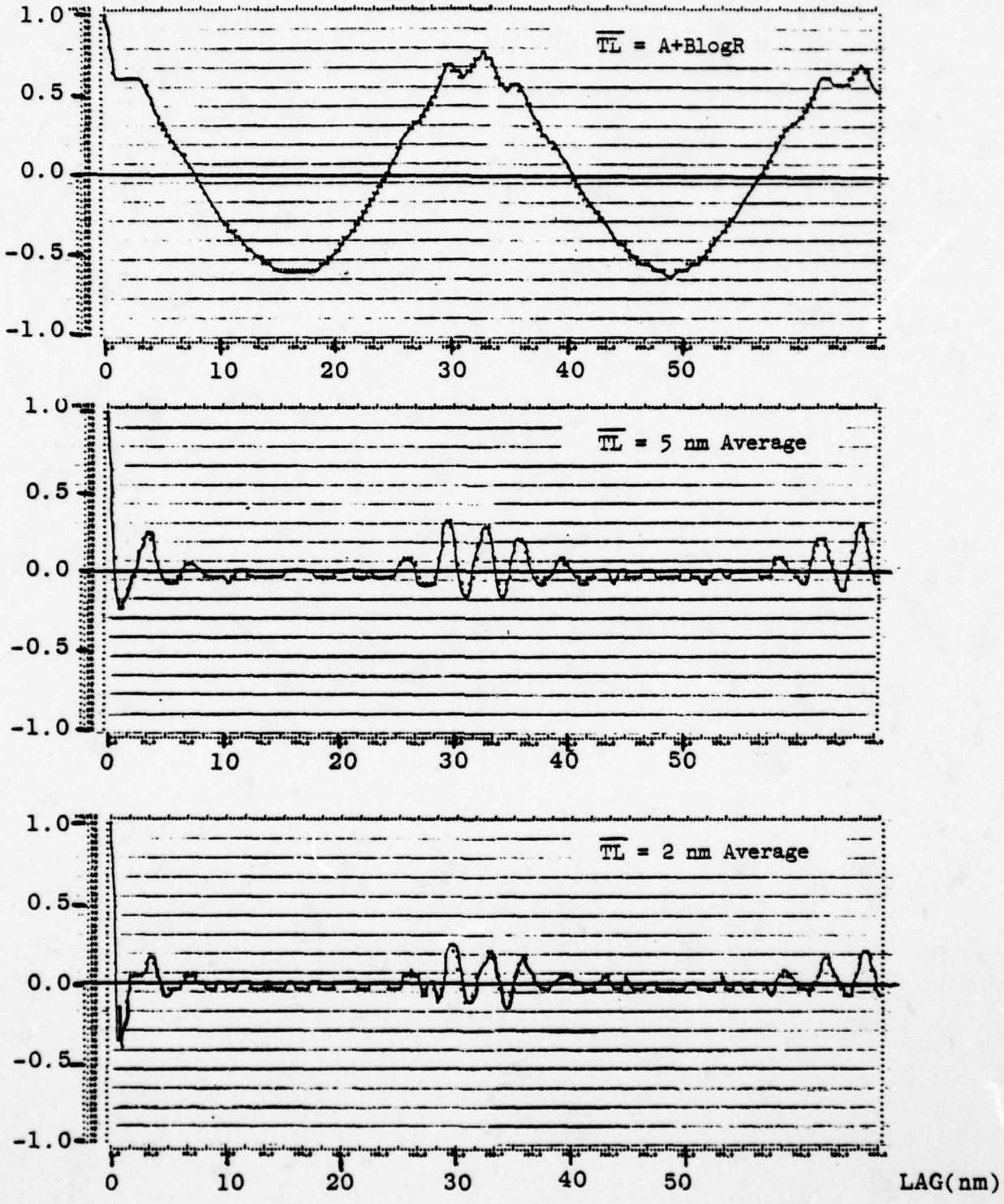

Autocovariance Functions for TL Fluctuations
Over Range Interval 100-500 nm

Figure 4-3

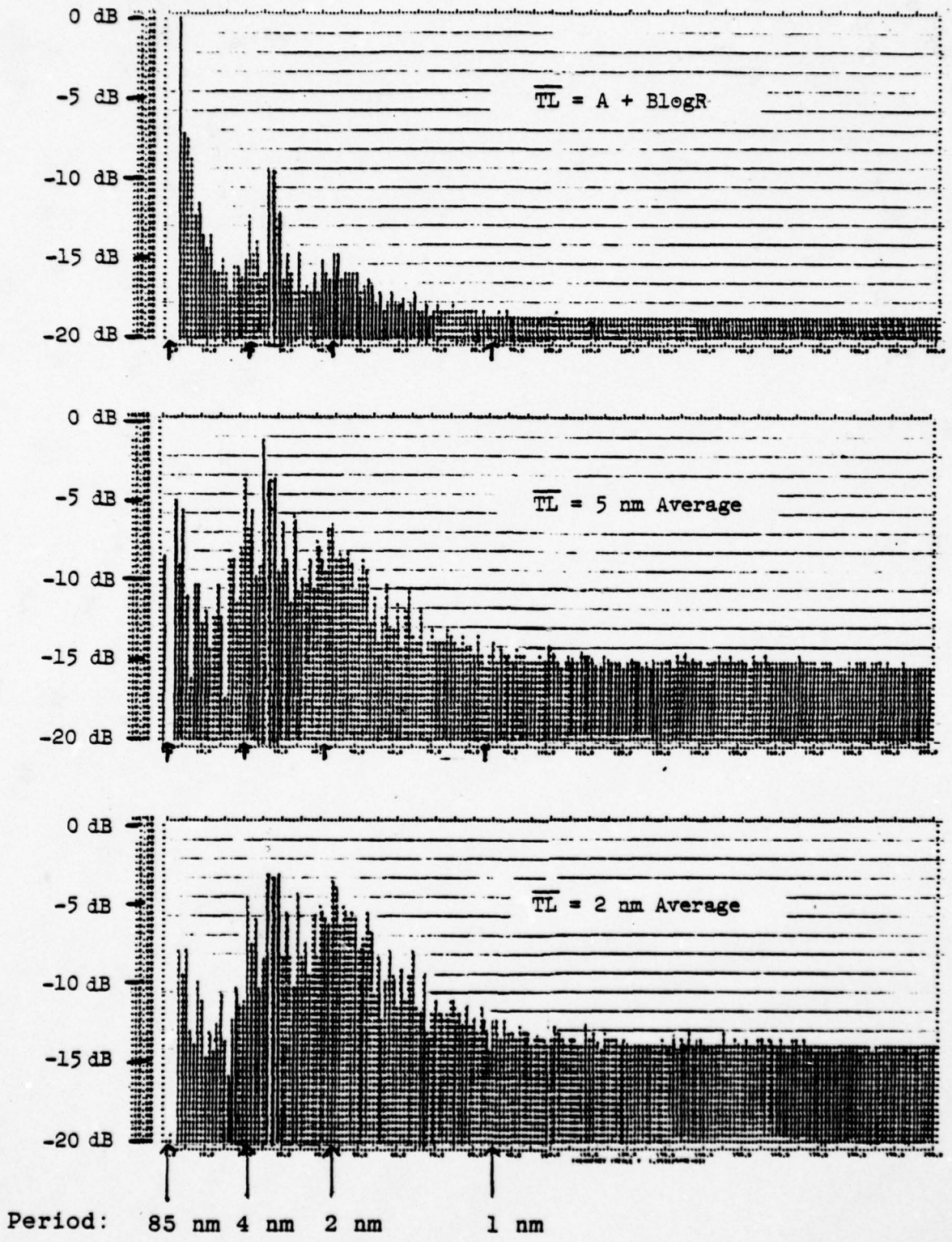

Spectra of TL Fluctuations -
Range Interval 100-500 nm

Figure 4-4

2 nm, plus strong low-frequency components (periods of 20^{+} nm). These two scales are consistent with the theory of multipath interference (Appendix D) for waterborne paths (small vertical angle apertures) and bottom bounce paths (wider aperture).

4.1.4 Level-Crossing Properties of TL

Some level-crossing properties of the total TL (not ΔTL) are summarized in Table 4-2 for the 100-500 nm interval and the 300 foot source (per Figure 4-1). Note that the data are "inverted" in the sense that for signal we usually look for properties of -TL rather than +TL as shown here. Also, the probabilities in the table are actually sample probabilities estimated from the 2400 data points.

If the three levels (99, 103, 107 dB) are viewed as FOM's and if the detector detects whenever the TL is less than the FOM, then the table shows that for a target with any range in 100-500 nm equally likely, there are average detection probabilities of 0.14, 0.44 and 0.74 for the three FOM's. The expected waiting ranges mean that if the target range is chosen at random in 100-500 nm, and the target is opening, then the waiting time to cross the level L is on the average 31, 1.8 or 0.3 nm, respectively. The small standard deviations indicate that there is not much variation about these average numbers.

Table 4-3 displays the distribution of range intervals during which TL is always below (or above) a

Sample Probabilities for 2400 points	L=99 dB	L=103 dB	L=107 dB
P(TL>L)	0.86	0.56	0.21
Expected Wait for TL >L (nm)	0.4	1.8	5.5
Standard Deviation (nm)	0.1	0.3	0.5
P(TL>L			
at least once in interval of 1 nm)	0.91	0.71	0.35
at least once in interval of 2 nm)	0.94	0.78	0.45
at least once in interval of 3 nm)	0.95	0.81	0.52
at least once in interval of 4 nm)	0.96	0.84	0.56
at least once in interval of 5 nm)	0.97	0.85	0.60
P(TL<L)	0.14	0.44	0.79
Expected Wait for TL<L (nm)	31.0	1.8	0.3
Standard Deviation (nm)	1.1	0.3	0.1

Some Level-Crossing Properties
of TL Over Range Interval 100-500 nm

Table 4-2

k(nm)	L = 99 dB		L = 103 dB		L = 107 dB	
0.16 - 0.2	2	(1)	12	(3)	1	(12)
0.2 - 0.5	1	(0)	3	(3)	3	(5)
0.5 - 1.0	9	(6)	30	(20)	24	(23)
1 - 2	6	(6)	30	(34)	20	(17)
2 - 4	4	(3)	7	(13)	7	(10)
4 - 10	3	(0)	0	(7)	6	(3)
10 - 16	0	(0)	2	(0)	1	(0)
16 - 32	0	(8)	4	(6)	8	(0)
32 - 48		(0)				
48 - 100		(0)				
> 100		(1)				

Number of Intervals of Length k for which TL<L (TL>L)

Level-Crossing Properties of Acoustically Modeled TL:
Distribution of Interval Lengths
Over Ranges 100-500 nm

Table 4-3

level L, as measured over the 400 nm track from 100-500 nm. The interpretation depends on the way in which intervals are counted: an interval of length k miles is one for which TL<L (or >L) for exactly k miles and no more. The table then shows the number of intervals within a window of lengths. For example, at L = 99 dB, there are:

- 2 intervals with lengths between 0.16 and 0.2 nm for which TL≤L
- 9 intervals with lengths between 0.5 and 1.0 nm for which TL≤L
- 6 intervals with lengths between 0.5 and 1.0 nm for which TL>L.

As noted in Appendix A,

$$P(TL \leq L) \simeq \left(\frac{\sum_{k} (\text{Number of Intervals of Length k with } TL \leq L)(k)}{400 \text{ nm}} \right), \quad (4\text{-}1)$$

so that the distribution of interval lengths is constrained by more than the decorrelation range.

Some observations about values shown in the table follow.

- Symmetry of the distributions corresponding to TL>103 and TL<103 is suggested. This might be expected since P(TL>103) is near 0.5. However, there are indeed more long intervals with TL>L and more short ones with TL≤L, and the reason is that the TL fluctuations are skewed - with deep fades

about the mean (TL>>L) but only small excursions of TL<L. This is apparent in the waiting times of Table 4-2 as well.

- Similarly, differences in the distributions of interval lengths for TL>99 and TL<107, as well as for TL<99 and TL>107, are attributed to the tendency of transmission toward large fades.

- All of the distributions are concentrated at interval lengths between 0.5 and 2 nm. Although a decorrelation range of about 5 nm is appropriate for the total TL over the 100-500 nm interval (from the A+BlogR fit), the faster fluctuations seem to have a significant influence on the level-crossing properties.

- Given this concentration of interval lengths, the principal difference between one distribution and another is driven by the number of long intervals. Equation (4-1) shows how a single long interval displaces many short ones.

These features will become important when the stochastic data are compared with the acoustic data in the next section.

4.2 Basic Properties of Stochastically Modeled TL

The statistical properties of the stochastic processes considered in this study were summarized in Section 3. Since each process is ergodic, after a sufficient amount of time, the time-sampled statistical properties will approximate the ensemble properties. For example, if the process has a normal marginal distribution, then a histogram constructed from a sample path (realization) will approach that distribution as the duration of the time series increases.

Even though most of the properties are known, it seems worthwhile to summarize the results for 40 replications of the GM and Jump processes corresponding to the long-range TL fluctuations of 4.1. The purpose is to compare the stochastic and acoustic time series, and to thus illustrate some effects of finite sampling and the differences between processes. Along with the TL fluctuation properties, the level-crossing statistics of TL simulations ($\overline{TL}$ + Random Process) will be displayed. All of this is used to judge the adequacy of the stochastic-process models to simulate TL and its fluctuations as functions of average $\overline{TL}$.

4.2.1 Sample Functions of TL Fluctuations

As an aid to visualizing the differences between the Jump and GM processes, Figure 4-5 shows typical sample functions of each. They correspond to the parameters (μ, σ, τ) found above for TL fluctuations over the 100-500 nm interval, and for the 2 nm average and A+BlogR fit for $\overline{TL}$. For the A+BlogR fit, (μ, σ, τ) = (0.0, 5.0, 4.7 nm), and the two sample functions clearly exhibit the special character of their parent processes, the step versus continuous sample paths. The number of jumps is 25 out of a total of 1000 sample points for the Jump process - consistent with the value of τ (one jump every 4.7 nm or 28 points). To the more detailed $\overline{TL}$ (2 nm), there corresponds a tighter fluctuation distribution, (μ, σ, τ) = (0.6, 2.2, 0.5 nm), and the GM and Jump processes begin to look more alike (in the limit of τ = 0, they are the same).

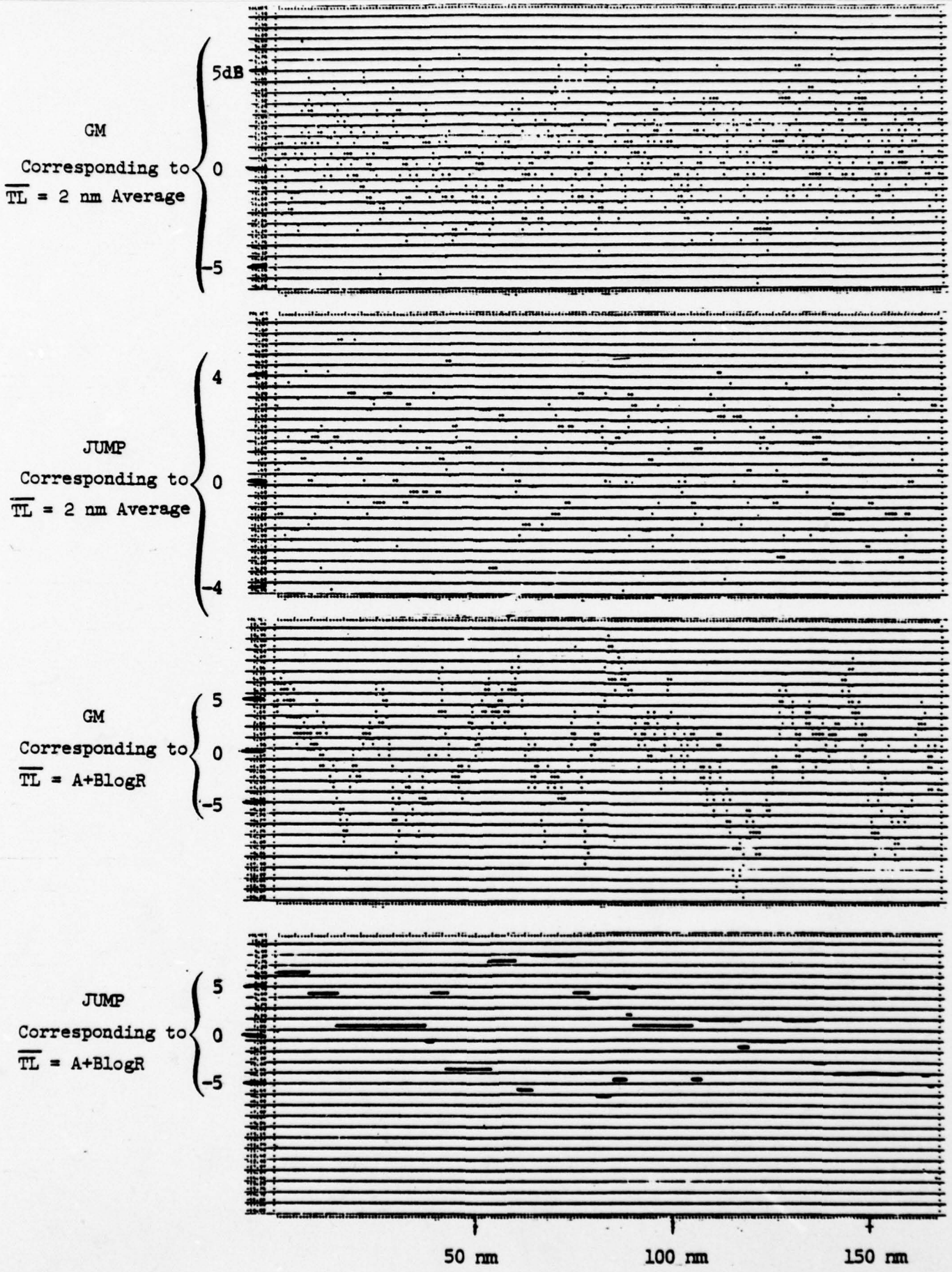

Figure 4-5 Simulated TL Fluctuations

Comparison of the sample paths of Figure 4-5 with those of Figure 4-2 suggests that the GM process better mimics the character of the acoustic simulations, but that for τ small (detailed $\overline{TL}$) the Jump process may also be quite satisfactory.

4.2.2 Sample Moments and Distribution Functions

Sample mean, standard deviation, skewness, and kurtosis were calculated for the simulated TL fluctuations described in the preceding paragraph and are displayed in Table 4-4. The "long-term" and ensemble values of these statistics are known, but it is instructive to notice that the subinterval moments make the (stationary) GM and Jump processes look even more non-stationary than the acoustically-modeled fluctuation process. This is, of course, a vagary of sampling: the observed values are within expected limits corresponding to the number of independent samples making up the statistics. (The decorrelation times shown in the same figure are used to estimate the "effective" number of "independent" samples). Ensemble statistics were also calculated for 40 replications of the stochastic processes; they look much the same as the time statistics and are not displayed.

The sample distribution functions were calculated for 40 replications of the processes. As expected, when the number of independent samples is properly estimated (using decorrelation and zero-crossing times), the sample functions are accepted at the 0.05 or higher significance levels as normal (i.e., log-normal intensities) with a Lilliefors version of the Kolmogorov test. This

	GM Corresponding to $\overline{TL}$ = A + BlogR (μ=0.0; σ=5.0; τ=4.7 nm)				JUMP Corresponding to $\overline{TL}$ = A + BlogR (μ=0.0; σ=5.0; τ= 4.7 nm)			
	Statistics (dB)				Statistics (dB)			
	μ	σ	skewness	kurtosis	μ	σ	skewness	kurtosis
100-200 nm	0.4	4.5	- .2	-.5	2.2	4.4	- .2	- .9
200-300	- .6	4.8	- .4	-.2	- .8	4.6	-1.1	6.2
300-400	-2.4	5.0	0.1	-.1	0.0	4.2	-1.2	1.9
400-500	-1.9	3.9	- .2	-.1	-2.3	3.2	1.1	1.8
100-300	- .1	4.6	- .3	- .3	.7	4.7	- .6	3.0
300-500	-2.1	4.4	0.0	0.1	-1.1	3.9	- .2	0.6
100-500	-1.1	4.7	- .1	-.2	-0.2	4.4	- .4	2.0
Decorrelation Range and Range to First Zero-Crossing of Auto-covariance (nm)	4 8.5				3.3 19			
Effective Number of "Independent" Points Over 100-500 nm (out of 2400 points)	100				130			

	GM Corresponding to 2 nm Average $\overline{TL}$ (μ=0.6; σ=2.2; τ=0.5 nm)				JUMP Corresponding to 2 nm Average $\overline{TL}$ (μ=0.6; σ=2.2; τ=0.5 nm)			
	Statistics (dB)				Statistics (dB)			
	μ	σ	skewness	kurtosis	μ	σ	skewness	kurtosis
100-200 nm	0.3	2.0	0.2	- .3	0.4	2.0	- .2	- .4
200-300	0.7	2.2	0.0	0.0	0.3	2.3	0.2	- .3
300-400	0.6	2.3	- .1	0.4	0.8	2.2	0.1	0.1
400-500	0.4	2.0	- .1	- .2	0.4	2.1	0.0	- .3
100-300	0.5	2.1	0.1	- .2	0.3	2.2	0.0	- .3
300-500	0.5	2.2	- .1	0.2	0.6	2.2	0.1	- .1
100-500	0.5	2.1	0.0	0.0	0.5	2.2	0.0	- .2
Decorrelation Range and Range to First Zero-Crossing of Auto-covariance (nm)	0.5 1.7				0.7 1.7			
Effective Number of "Independent" Points Over 100-500 nm (out of 2400 points)	800				600			

Statistics for a Typical TL Simulation
Over Range Interval 100-500 nm

Table 4-4

is of course one major discrepancy between the acoustic and stochastic simulations - since the acoustic TL fluctuation distributions were rejected as normal for the detailed $\overline{TL}$. We note also that the stochastic process simulations often passed the Kolmogorov test at the 0.01 level for the high d.f. chi-square intensity distribution. The reason is that any Gaussian-like haystack density function looks log-normal near the mean.

4.2.3 Correlation Properties

Normalized autocovariance functions for the four sample functions described above are shown in Figure 4-6. Again, note that the GM and Jump samples are typical of the many which were generated for this study. The plots show the expected exponential decay. The observed decorrelation ranges are near those used as input to the random process generator (see Table 4-3). The sample covariance functions become "noisy" for lags beyond about 10% of the total range of observation (400 nm).

The difference in correlation properties between the stochastic and acoustic simulations is apparent when the curves of Figure 4-6 are compared with those of Figure 4-3. However, a better appreciation can be gained when the corresponding Fourier transforms ("spectra") of Figures 4-7 and 4-4 are compared. The spectra for the stochastic processes are as expected for an exponential autocovariance function: they have the proper shape (from Table 3-1):

$$S(\omega) = \frac{2\lambda}{\omega^2 + \lambda^2}, \quad \omega = 2\pi f, \quad \lambda = 1/\tau,$$

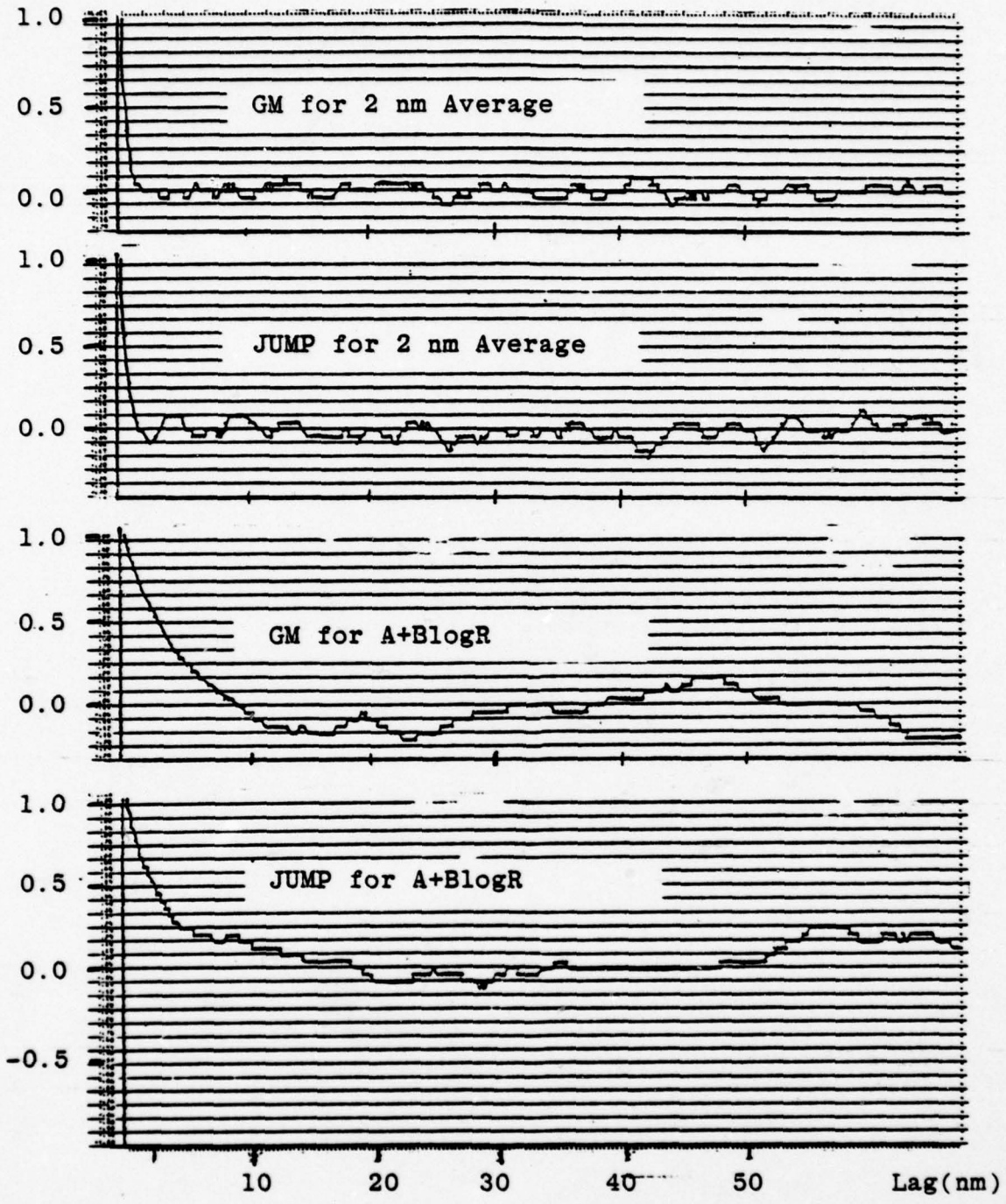

Autocovariance Functions for Simulated TL Fluctuations
(Over Range Interval 100-500 nm)

Figure 4-6

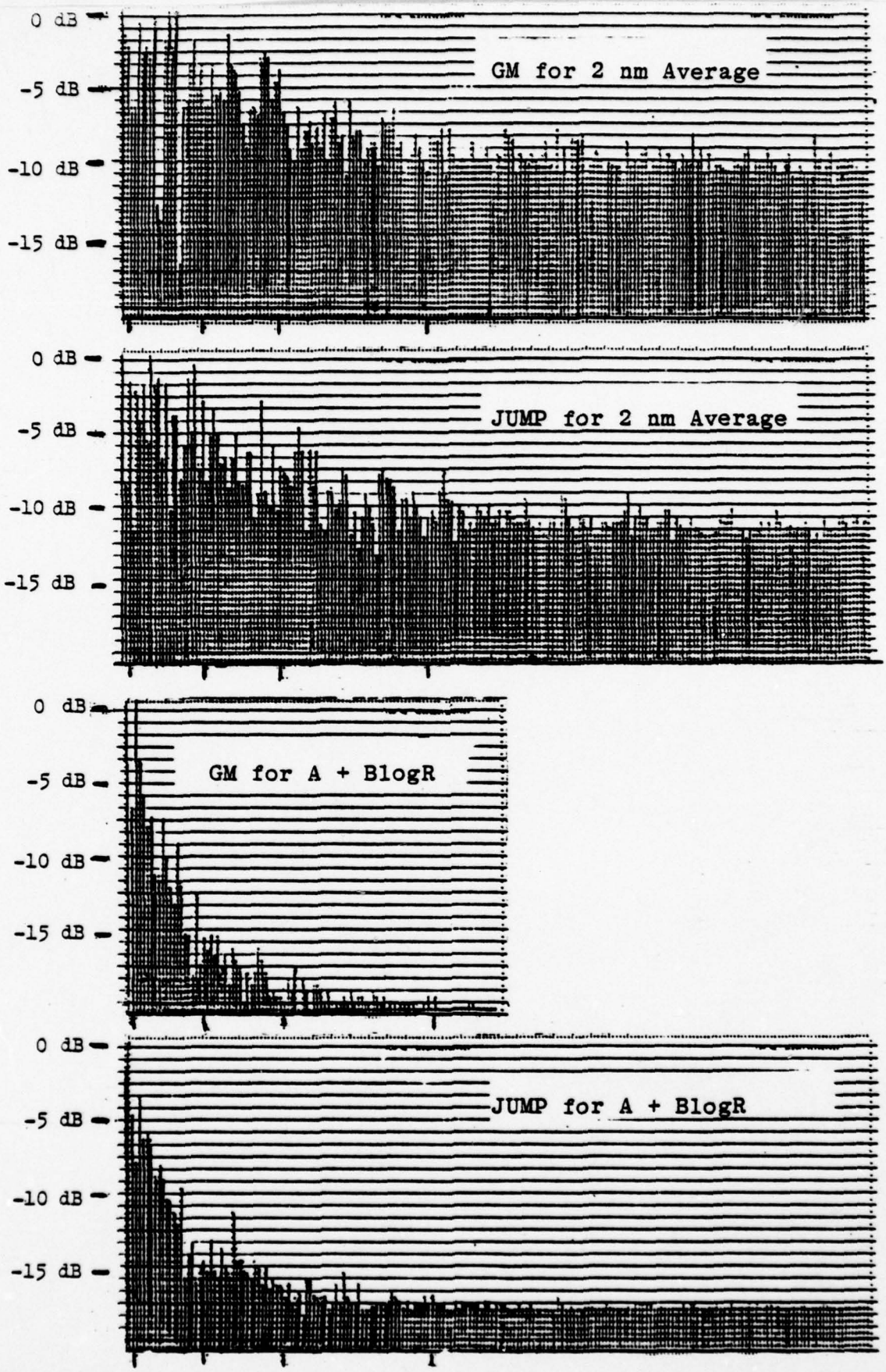

Figure 4-7 Spectra of TL Fluctuations (see Figures 4-5 and 4-6) (Over 100-500 nm Interval)

with

3 dB-down points at frequencies with periods: $2\pi\tau$,

6 dB-down points at frequencies with periods: $\pi\tau$,

10 dB-down points at frequencies with periods: $2\pi\tau/3$.

These three range-periods are about 30, 15, and 10 nm for the $\overline{TL} = A+B\log R$ case ($\tau \approx 5$ nm) and about 3, 1.5, and 1 nm for the 2-mile-average case ($\tau \approx 0.5$ nm). The spectra for the acoustically modeled TL fluctuations (Figure 4-4) are not at all similar to these, and the same observation holds for simulations over other range intervals.

This second discrepancy between properties of the two types of models can be summarized as follows.

- Whereas the stochastic simulations display exponentially decaying autocovariance functions and their monotone, smooth spectra, the acoustically modeled data show significant structure in the autocovariance functions (resembling a damped cosine) and spectra with "power" concentrated at preferred fluctuation periods (e.g., 1 to 5 nm).

4.2.4 Level-Crossing Properties for TL(R)

The level-crossing statistics of the stochastic TL simulations were obtained from samples of simulated $\hat{TL}(R)$ generated as

$$\hat{TL}(R) = \overline{TL}(R) + \Delta\hat{TL}(R)$$

over $100<R<500$ nm with $\overline{TL}$ either (A+BlogR) or a 2-mile average and $\Delta\hat{TL}(R)$ the appropriate GM or Jump process (i.e., the same cases focussed on throughout this section). For 40 replications of the 400 nm range-series of $\hat{TL}$, the statistics were calculated for comparison with those of the acoustic TL(R) (displayed in Table 4-2). These level-crossing statistics are summarized in Tables 4-5 and 4-6 with the 20^{th}, 50^{th}, and 80^{th} percentile values of $P(\hat{TL}<L)$, $P(\hat{TL}>L)$, and expected waiting "times." In the same tables are displayed the corresponding acoustically modeled statistics (from Table 4-2).

- The results for $\overline{TL}$ = (A+BlogR) show a wide range of values from the 20th to 80th percentile, and the best agreement is for the Jump process.
- For the 2-mile average $\overline{TL}$, the range of values is much smaller and the Jump process again shows best agreement with the acoustic data. In fact, except for the waiting time for TL<99 dB, the median values* are very close to the statistics for the acoustic data.

Table 4-7 shows distributions of interval lengths for which TL is less than L. These are based on "typical" replications, and in fact the general properties of these statistics were quite consistent from one sample function to another. The corresponding data for the acoustically modeled TL (from Table 4-3) are given in the same table, and a comparison shows:

*Note that the median values are in good agreement with the analytic level-crossing solutions for the Jump process with a constant threshold (very nearly the case for $\overline{TL}$ = A+BlogR), as given by formulas (3-1) and (3-2) of Table 3-1.

Property	Simulation	L = 99 dB	L = 103 dB	L = 107 dB
P(TL<L)	GM + 2-mile avg.	.13/.14/.14*	.38/.41/.42	.76/.76/.78
	Jump + 2-mile avg.	.13/.14/.15	.39/.40/.41	.74/.76/.77
	GM + A+BlogR	.10/.18/.20	.36/.50/.51	.65/.69/.82
	Jump + A+BlogR	.12/.13/.16	.32/.42/.45	.70/.73/.78
	Acoustic	0.14	0.44	0.79
Expected Wait for TL<L (nm)	GM + 2-mile avg.	9/11/14	1.8/2.0/2.4	0.3/0.4/0.4
	Jump + 2-mile avg.	12/16/21	2.0/2.4/2.7	0.4/0.5/0.5
	GM + A+BlogR	7/9/14	1.5/2.9/5.0	0.2/0.7/1.1
	Jump + A+BlogR	22/29/42	6/6/13	0.7/1.4/2.3
	Acoustic	31	1.8	0.3
Expected Wait for TL>L (nm)	GM + 2-mile avg.	0.2/0.3/0.3	1.1/1.3/1.3	4.0/4.5/5.0
	Jump + 2-mile avg.	0.2/0.3/0.4	1.3/1.4/1.6	4.0/5.0/5.2
	GM + A+BlogR	0.2/0.3/0.4	1.1/1.5/2.2	4.7/4.7/5.3
	Jump + A+BlogR	0.6/0.8/1.1	3.2/3.7/4.0	10/11/12
	Acoustic	0.4	1.8	5.5

* 20th, 50th, and 80th Percentile Values from 40 Sample Paths of 2400 Points, Over 100-500 nm.

Stochastically Modeled Level-Crossing Statistics of TL
Compared to Acoustic Data (from Table 4-2)

Table 4-5

Property	Simulation	L = 99 dB	L = 103 dB	L = 107 dB
P(TL≥L at least once in 1-mile interval)	GM + 2-mile avg.	.92/.93/.94*	.77/.77/.77	.39/.41/.41
	Jump + 2-mile avg.	.93/.93/.93	.73/.74/.75	.34/.38/.42
	GM + A+BlogR	.88/.91/.95	.62/.68/.76	.31/.43/.47
	Jump + A+BlogR	.86/.88/.89	.58/.61/.71	.25/.30/.34
	Acoustic	0.91	0.71	0.35
P(TL≥L at least once in 3-mile interval)	GM + 2-mile avg.	.95/.96/.97	.85/.85/.86	.55/.56/.56
	Jump + 2-mile avg.	.96/.97/.97	.82/.82/.83	.48/.50/.57
	GM + A+BlogR	.94/.97/.97	.72/.78/.85	.44/.56/.57
	Jump + A+BlogR	.88/.91/.91	.64/.68/.75	.31/.35/.40
	Acoustic	0.95	0.81	0.52
P(TL≥L at least once in 5-mile interval	GM + 2-mile avg.	.98/.98/.99	.90/.91/.92	.67/.69/.70
	Jump + 2-mile avg.	.98/.99/.99	.87/.88/.89	.60/.62/.69
	GM + A+BlogR	.98/.99/1.0	.84/.90/.92	.60/.67/.69
	Jump + A+BlogR	.91/.93/.94	.72/.75/.79	.41/.43/.49
	Acoustic	0.97	0.85	0.60

* 20th, 50th, and 80th Percentile Values from 40 Sample Paths of 2400 Points, Over 100-500 nm.

Stochastically Modeled Level-Crossing Statistics of TL
Compared to Acoustic Data (from Table 4-2)

Table 4-6

	Simulation	Interval Length k(nm) 0.16–0.2	0.2–0.5	0.5–1.0	1–2	2–4	4–10	10–16	>16
L = 99 dB	Log Fit + Jump	1	1	0	1	1	0	3	0
	2-mile Avg + Jump	9	7	12	11	5	2	0	0
	Log Fit + GM	18	8	8	9	2	1	0	0
	2-mile Avg + GM	34	6	12	6	3	3	0	0
	Acoustic	2	1	9	6	4	3	0	0
L = 103 dB	Log Fit + Jump	1	0	1	2	2	6	6	2
	2-mile Avg + Jump	15	15	23	15	11	6	3	0
	Log Fit + GM	33	7	24	11	9	6	7	0
	2-mile Avg + GM	18	26	35	26	11	6	3	0
	Acoustic	12	3	30	30	7	0	2	4
L = 107 dB	Log Fit + Jump	0	1	0	0	2	3	4	8
	2-mile Avg + Jump	12	10	12	16	10	11	2	7
	Log Fit + GM	26	4	10	21	10	10	4	4
	2-mile Avg + GM	47	17	17	22	10	12	7	3
	Acoustic	1	3	24	20	7	6	1	8

Number of Intervals of Length k with TL≤L

Level-Crossing Properties of Acoustically Modeled TL:
Distribution of Interval Lengths
Over Ranges 100-500 nm

Table 4-7

- The GM and Jump processes are readily distinguishable by their level-crossing results for short interval lengths. For intervals greater than the decorrelation range, they show similar behavior.

- The GM process, for either smoothed $\overline{TL}$, consistently overestimates the number of short intervals.

- The Jump process added to $\overline{TL} = A+B\log R$ generally overestimate the number of long intervals.

- The best match over all cases is given by the sum of the 2-mile average $\overline{TL}$ and the Jump process. The agreement is not very good - and this seems to be attributable to the lack of concentration of interval lengths between 0.5 and 2 nm. In light of equation (4-1) and the discussion of 4.1.4, the random-process models with their exponential autocovariance functions and symmetric distribution functions yield sample paths with too many short intervals and too few medium-length intervals.

In conclusion, the level-crossing properties of the acoustically-modeled TL over a long range interval (100-500 nm) are simulated moderately well by the Jump process added to a 2-mile intensity-averaged $\overline{TL}$. No other combination of $\overline{TL}$ and ΔTL is a very close second. Another test, over shorter range intervals but for signal-to-noise ratios, is given in Section 7.

4.3 Summary

Acoustically modeled TL as a function of range (R) is treated as a sum of two components: the trend, $\overline{TL}(R)$, and the fluctuation, $\Delta TL(R) = TL(R) - \overline{TL}(R)$.

Statistical properties of $\Delta TL(R)$ for various range intervals within 0 to 500 nm have been calculated for three types of smoothing: 2-mile intensity average, 5-mile average, A+BlogR fit.

The GM and Jump processes were used to simulate $\Delta TL(R)$, with input parameters (mean, variance, decorrelation time) determined directly from the acoustic data. Sample functions of $\widehat{\Delta TL}(R)$ were also added to $\overline{TL}$ to yield simulations of TL: $\widehat{TL} = \overline{TL} + \widehat{\Delta TL}$.

Highlights of the comparison of the acoustically and stochastically modeled TL are:

(i) The sample marginal density functions for the acoustic-intensity fluctuation data match a non-central or central chi-square density better than the log-normal of the stochastic process.

(ii) The sample autocovariance functions for the acoustic fluctuation data showed structure different from the exponential form of the stochastic models. Fourier transforms illustrate that fluctuation power occurs at preferred frequencies, in contrast to the stochastic-process models' smooth, monotone spectra.

(iii) Selected level-crossing properties of acoustically modeled TL itself were best fit with a simulation using a 2-mile average $\overline{TL}$ and

the Jump process. However, the agreement was only moderately good, with differences possibly attributable to (i) and (ii).

For signal modeling, the detection-related properties of TL are its level-crossing statistics. Hence, for the case at hand, the Jump-process fluctuation (given the proper inputs) added to the 2-mile average $\overline{TL}$ can yield a satisfactory simulation. The impact of inaccuracies in the simulation on performance predictions is discussed further in Section 7.

Section 5
ACOUSTICALLY MODELED OMNIDIRECTIONAL AMBIENT NOISE DATA

Fifty ten-hour and one thirty-five-hour replications of the acoustic noise model for the conditions given in Section 2 were run for the study of beam-noise modeling and detection. One of the byproducts is a set of omnidirectional noise time series, and it is profitable to examine these, both for comparison with the beam noise data given below and for verification that sidelobe levels are as modeled in Appendix G. No stochastic simulations of omni noise were tested.

On average there were 155 surface ships within the 500 nm radius which defines the ocean basin. Because of this large number of contributing sources, the noise is expected to be quite stable over time, and the statistics bear this out. Figures 5-1 and 5-2 show time-series records for two typical replications. In the first (called "Case 1"), a ship passes close to the receiver and perturbs the very stable field for several hours. The corresponding autocovariance function is nearly linear with a decorrelation time (τ) of about one hour. The spectrum shows only that the noise is dominated by a low-frequency trend (period of at least several hours). The mean is 83.7 dB and σ = 2.9 dB. The second case shows a number of perturbations by nearby or noisy ships, but no large excursions. The result is a mean of 83 dB, but a much

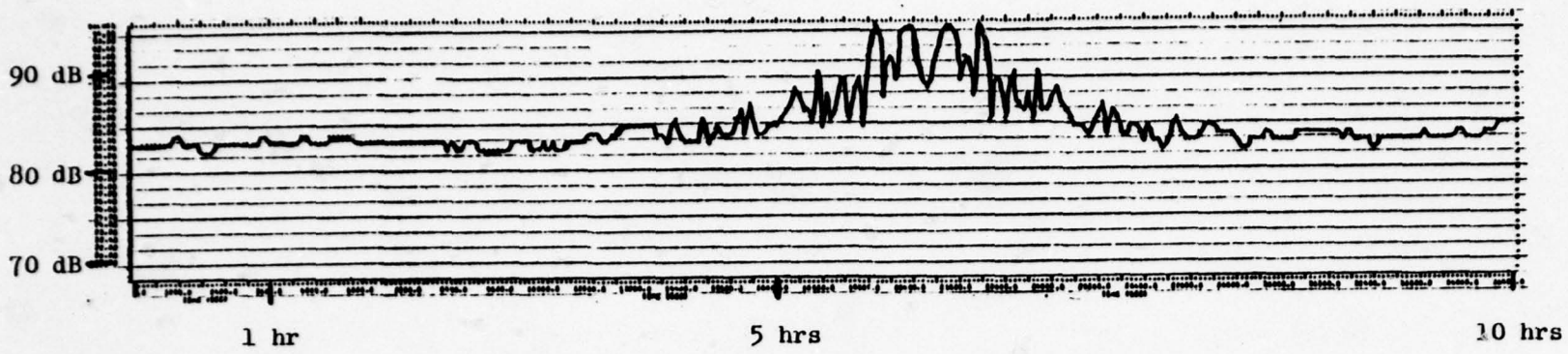

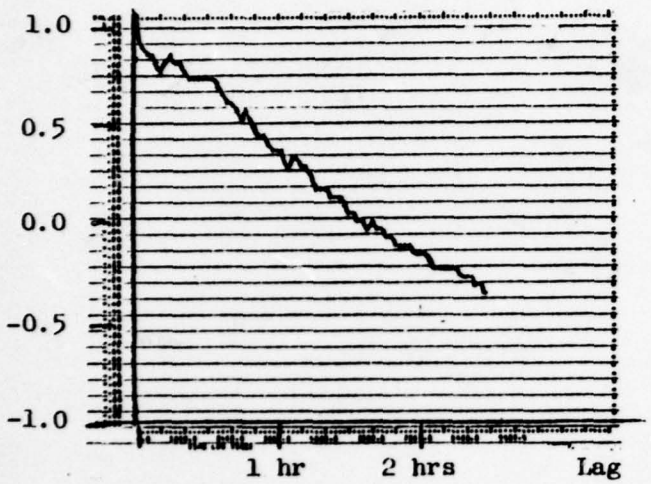

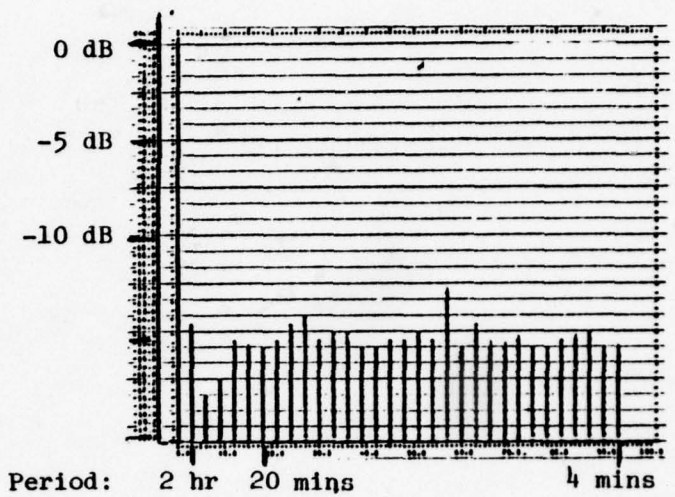

Time Series, Autocovariance, Spectrum of Typical Omni Noise Sample (#1)

Figure 5-1

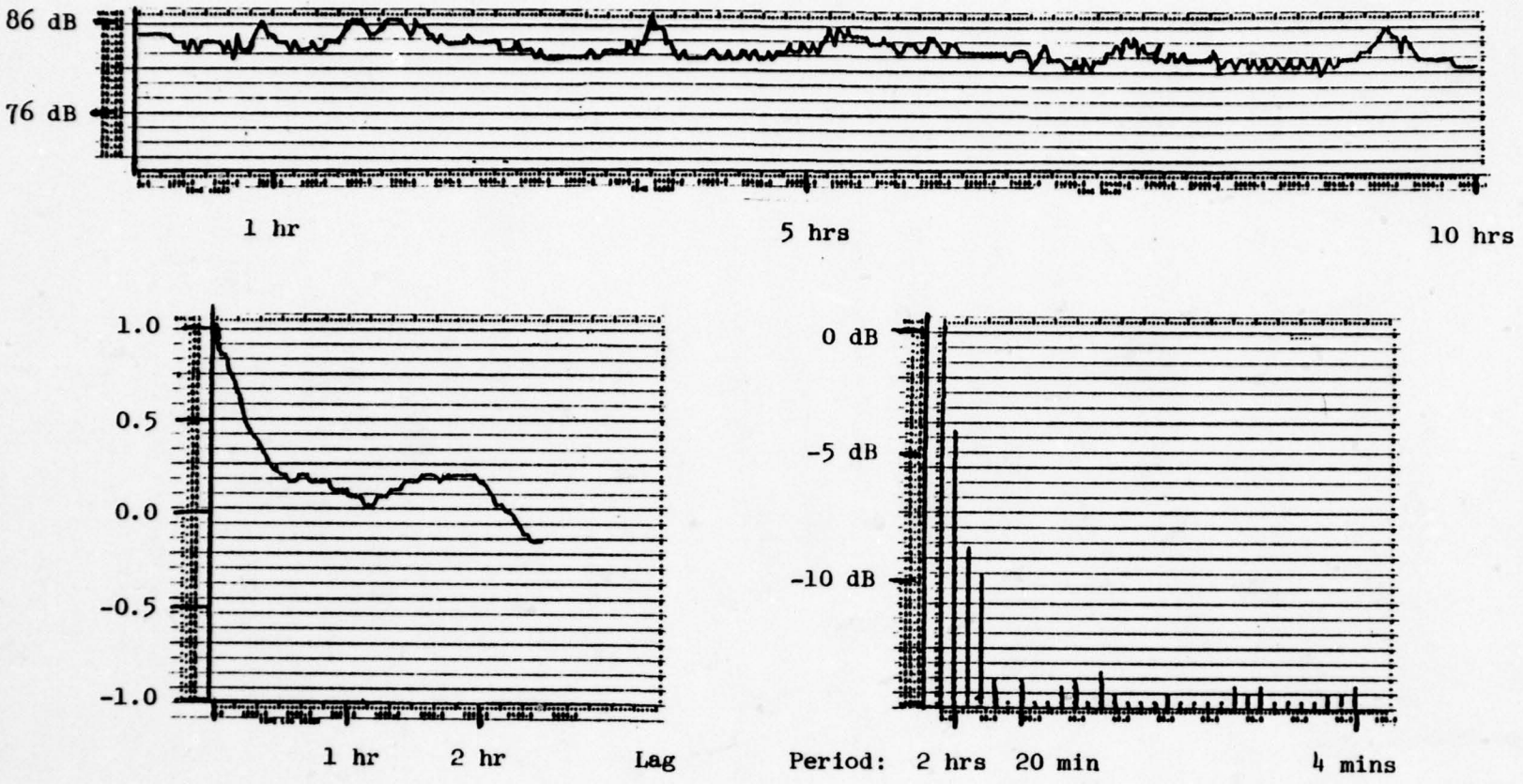

Time Series, Autocovariance, Spectrum of Typical Omni Noise Sample (#2)

Figure 5-2

smaller standard deviation (1.2 dB). The autocovariance function and spectrum of Figure 5-2 have a little more character, reflecting the semi-periodic occurrence of slightly higher levels every hour or so. Although the decorrelation time is about 20 minutes (as compared to an hour in Case 1), the first zero-crossing of the autocovariance function is beyond two hours here, as opposed to about 1.5 hours in the first case.

The large values of the decorrelation times indicate that moments or distribution functions obtained by time sampling over ten hours will be poor estimates, there may be as few as 5 or 10 "independent" samples. As a partial solution, we assume ergodicity and calculate moments at several fixed time points over the ensemble of 50 replications. The results are extremely consistent from time point to time point:

	Percentile		
	10	50	90
mean	83.3 dB	83.7	84
standard deviation	1.5 dB	2.1	2.8
skewness	.96	1.7	2.9
kurtosis	0.6	2.1	4.2

The implication is that the omni noise distribution has small variance and positive kurtosis. The skewness to the right is obviously the result of the occasional appearance of high noise levels from nearby or loud ships. In spite of the likelihood of undersampling, the sample density functions for Cases 1 and 2 above are shown in Figure 5-3, together with the densities for log transforms of

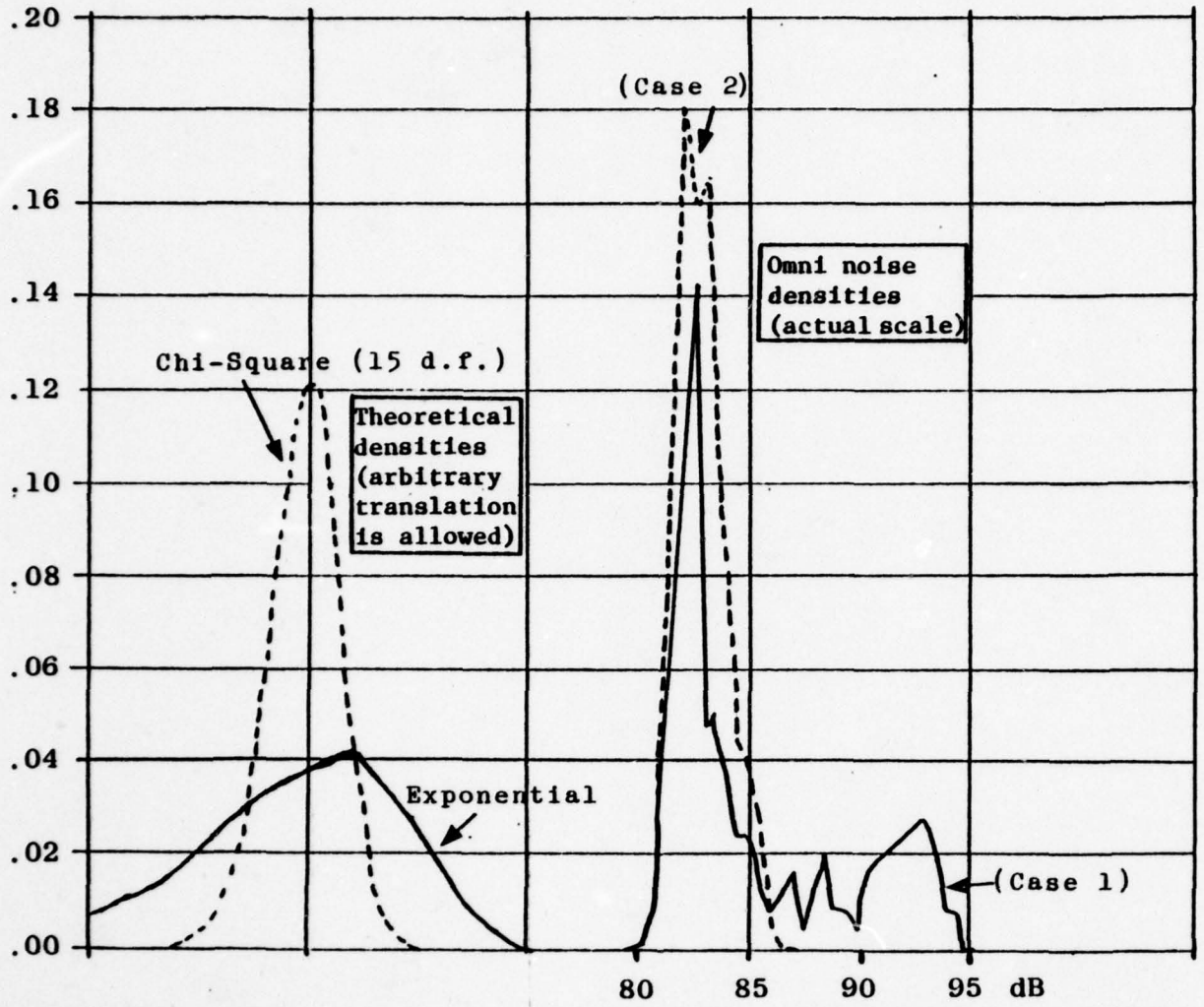

Sample Density Functions for Omni Noise Compared with Theoretical Densities
Figure 5-3

exponential and chi-square (15 d.f.) variables. The latter is a "best fit" for Case 2. While Case 1 is "bimodal" (as expected), Case 2 could pass as log-normal or chi-square, consistent with the theories presented in Appendix D.

Also note the variation from replication to replication of the decorrelation times of the omni noise times series:

	Percentiles		
	20	50	80
Decorrelation Time (mins)	20	25	60
First Zero-Crossing (mins)	40	95	130

Obviously, questions about long-term trends in noise will require much longer sample time series than are considered in this study.

There is one long replication of noise (35 hours), and it is encouraging to note that its covariance, spectrum and statistics (Figure 5-4, Table 5-1) are consistent with those of the 10 hour series. There is indeed little correlation beyond the first zero-crossing time and the long term statistics show the characteristic positive skewness.

In summary, omnidirectional ambient noise for a case in which many ships contribute is quite stable (σ over ten hours is typically less than 3 dB) with first order properties consistent from sample to sample (the mean ranged from 83 to 84 dB, the skewness from 1 to 3).

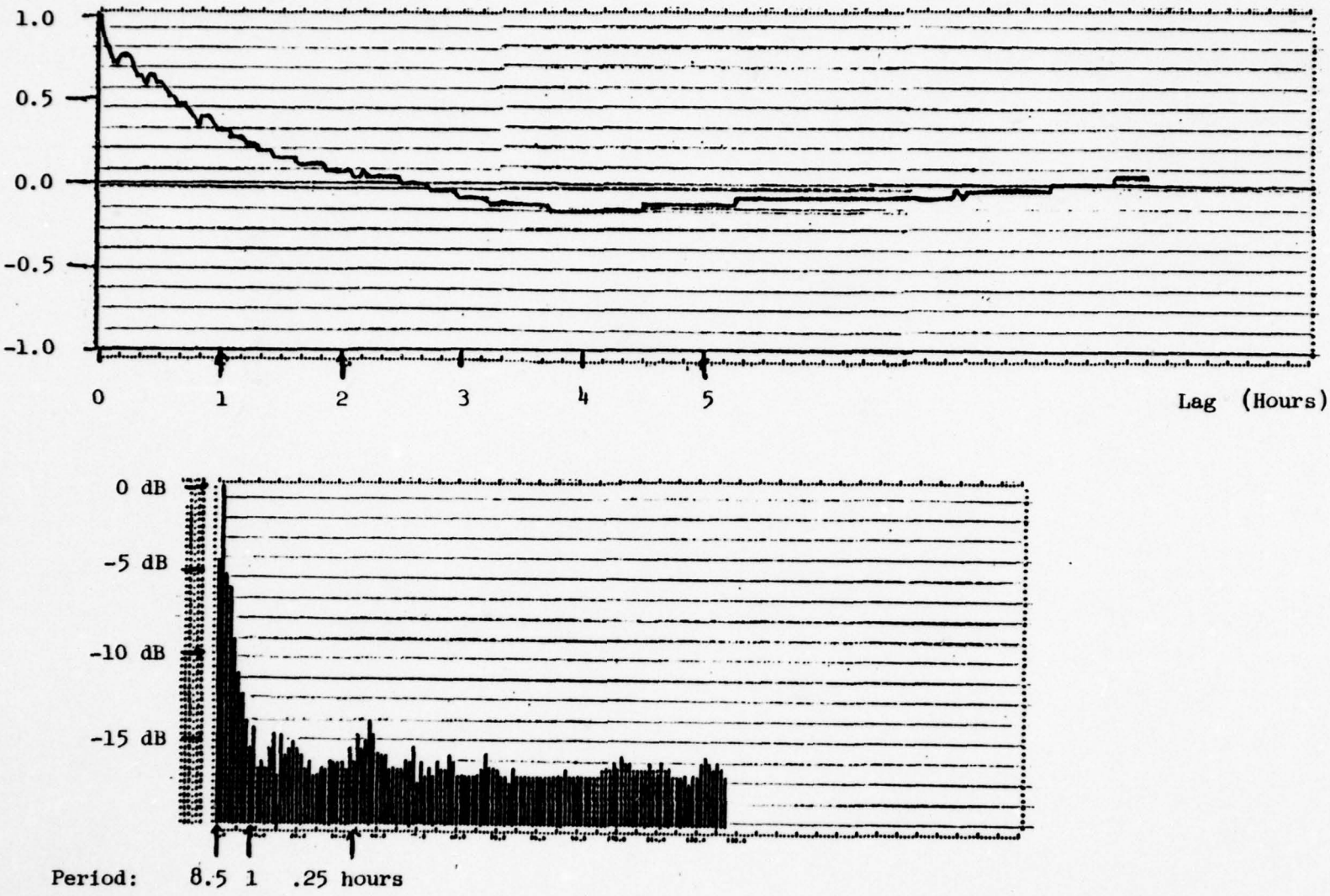

Autocovariance and Spectrum for 35-Hour Noise Series

Figure 5-4

Time Period (Hours)	Mean	Standard Deviation	Skewness
0.0 - 8.8	84.2 dB	3.2 dB	1.5
8.8 - 17.6	82.0	1.9	1.2
17.6 - 26.4	81.9	2.5	1.9
26.4 - 35.0	82.7	4.3	2.9
0.0 - 17.6	83.1	2.9	1.7
17.6 - 35.0	82.3	3.5	3.1
0.0 - 35.0	82.7	3.2	2.5

- Decorrelation Time = 56 minutes
- Time to First Zero-Crossing of Autocovariance = 156 minutes

Statistics for 35-Hour Omni Noise Time Series
Table 5-1

The decorrelation times are large and, in view of the small variance, not too important. It is observed that the principal uncertainty in predicting such noise properties is in estimating the time and duration of nearby ship "interference." Simple analytical models which might eliminate that problem are available.

Section 6

RESULTS FOR ACOUSTICALLY AND STOCHASTICALLY MODELED BEAM-NOISE FLUCTUATIONS

This section derives and compares the properties of acoustically and stochastically modeled beam noise, i.e., ambient noise as observed by the generic towed array system described in Subsection 2.2.

Before the results are presented, certain simplifications in the analysis should be noted. The array response is ideal, represented by a time-invariant beam pattern with a simple main lobe and uniformly suppressed sidelobes (see 2.2). As discussed in Appendix G, the choice of array steering angles near broadside makes multipath beam splitting unimportant, while the sidelobe suppression (30 dB or more) guarantees that noise sources off the main beam contribute little to the fluctuations.

Finally, recall that in the study of transmission loss, a predictable trend was removed and the residual became the fluctuating component. In the case of noise, however, only the long-term (e.g., 24 hours) mean is assumed to be predictable, so that any departure from the mean is treated as a fluctuation.

6.1 Properties of Acoustically Modeled Beam Noise

The acoustic beam-noise data were generated with the DSBN model described in Appendices C and H, and

used the TL, shipping and array-response inputs identified in Subsection 2.2.

Fifty realizations of DSBN beam noise, each of duration ten hours, were generated for this study. The model was run with independently selected ship parameters each time, and a few sample cross-correlations suggest that the 50 series can be treated as independent samples. The time series were themselves sampled at two minute intervals so that each realization consists of 300 time points. For each of the ten-hour DSBN series, outputs were obtained for eight array beams (Table 2-1) as well as the omnidirectional noise. There is also one long (35 hour) time series of noise, so that long-term trends can be investigated for at least one case.

6.1.1 Typical Beam-Noise Time Series

Begin by looking at two typical noise time series, the same two discussed in Section 5 as Case 1 and Case 2. Figures 6-1 and 6-2 show the time series for near-broadside beams with 8° beamwidth and 30 dB sidelobe suppression. Although the time scales resemble those for omnidirectional noise (Figures 5-1 and 5-2), the beam-noise data show much larger excursions. The reason is that there are on average 155 ship sources contributing to the omni noise, but only seven ships for the beam noise (8° beam and ambiguous image beam).

The complicated behavior of beam noise can be appreciated when the simultaneous outputs of three different beams (Case 2) are compared as in Figure 6-3.

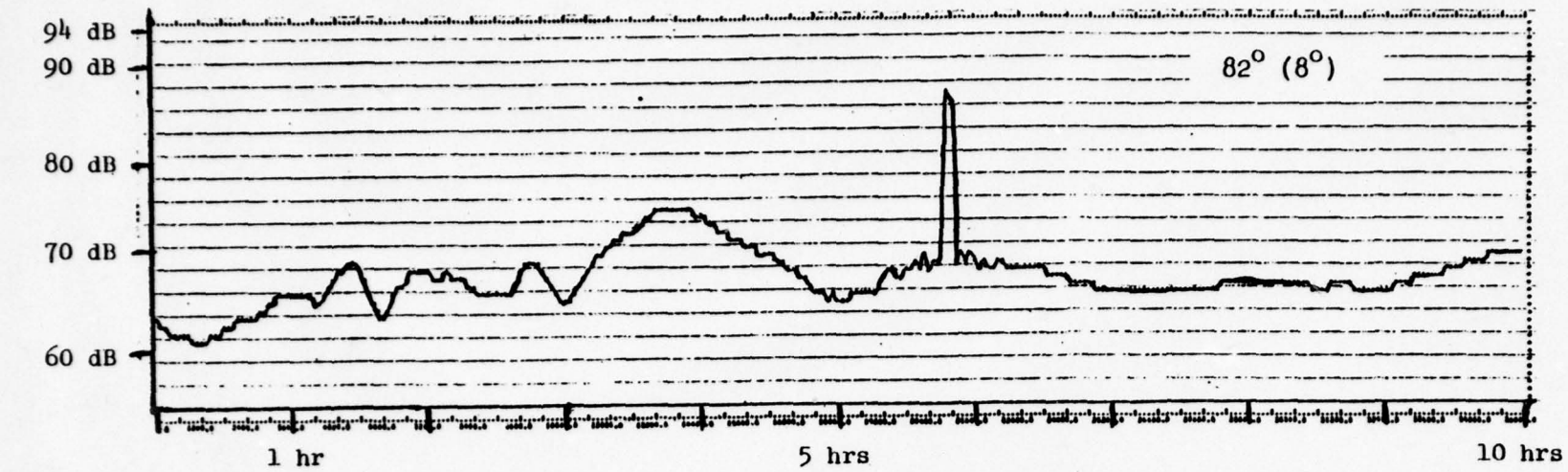

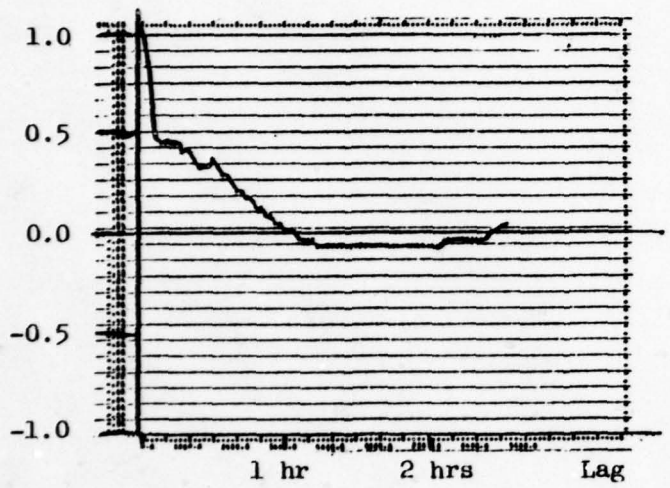

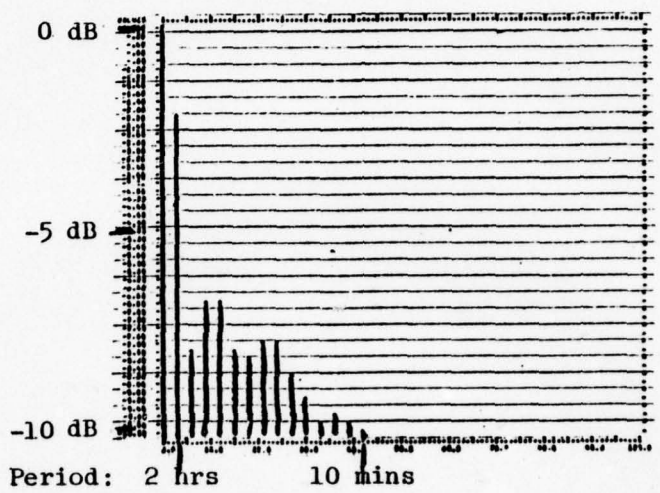

Time Series, Autocovariance and Spectrum for Beam Noise (Case #1)
82° Beam (8° T), 8° Beamwidth, 30 dB Sidelobe Suppression

Figure 6-1

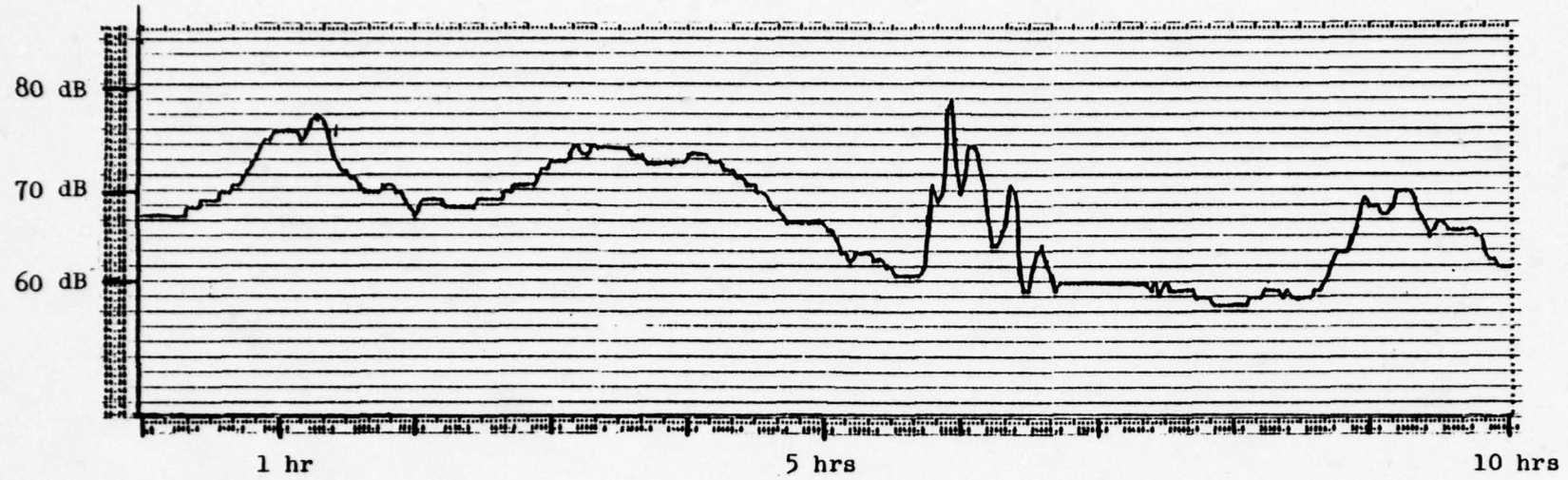

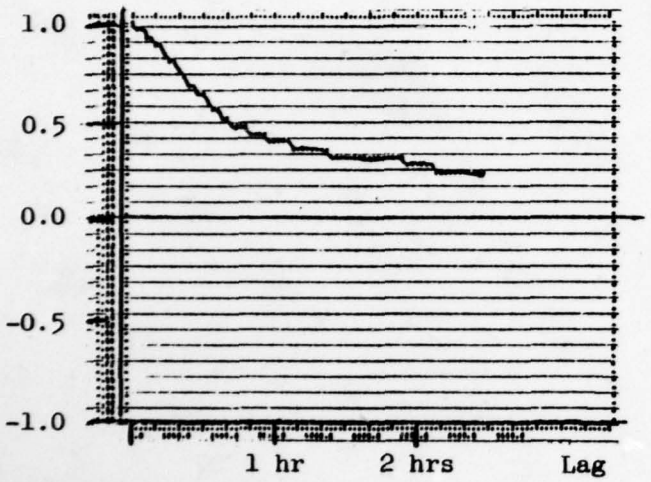

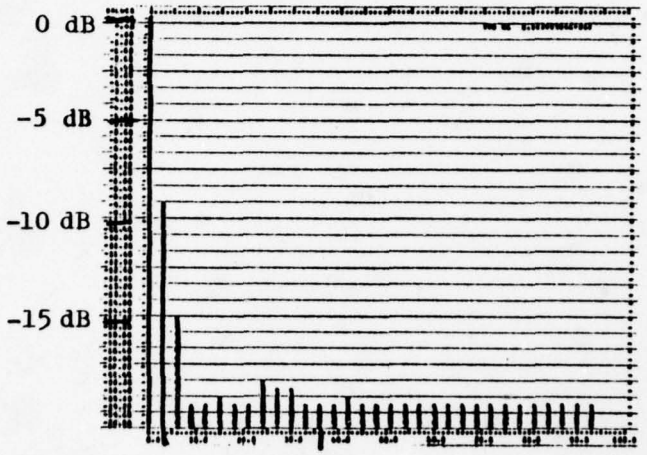

Time Series, Autocovariance, and Spectrum for Beam Noise (Case #2)
90^{O} Beam (0^{O} T), 8^{O} Beamwidth, 30 dB Sidelobe Suppression

Figure 6-2

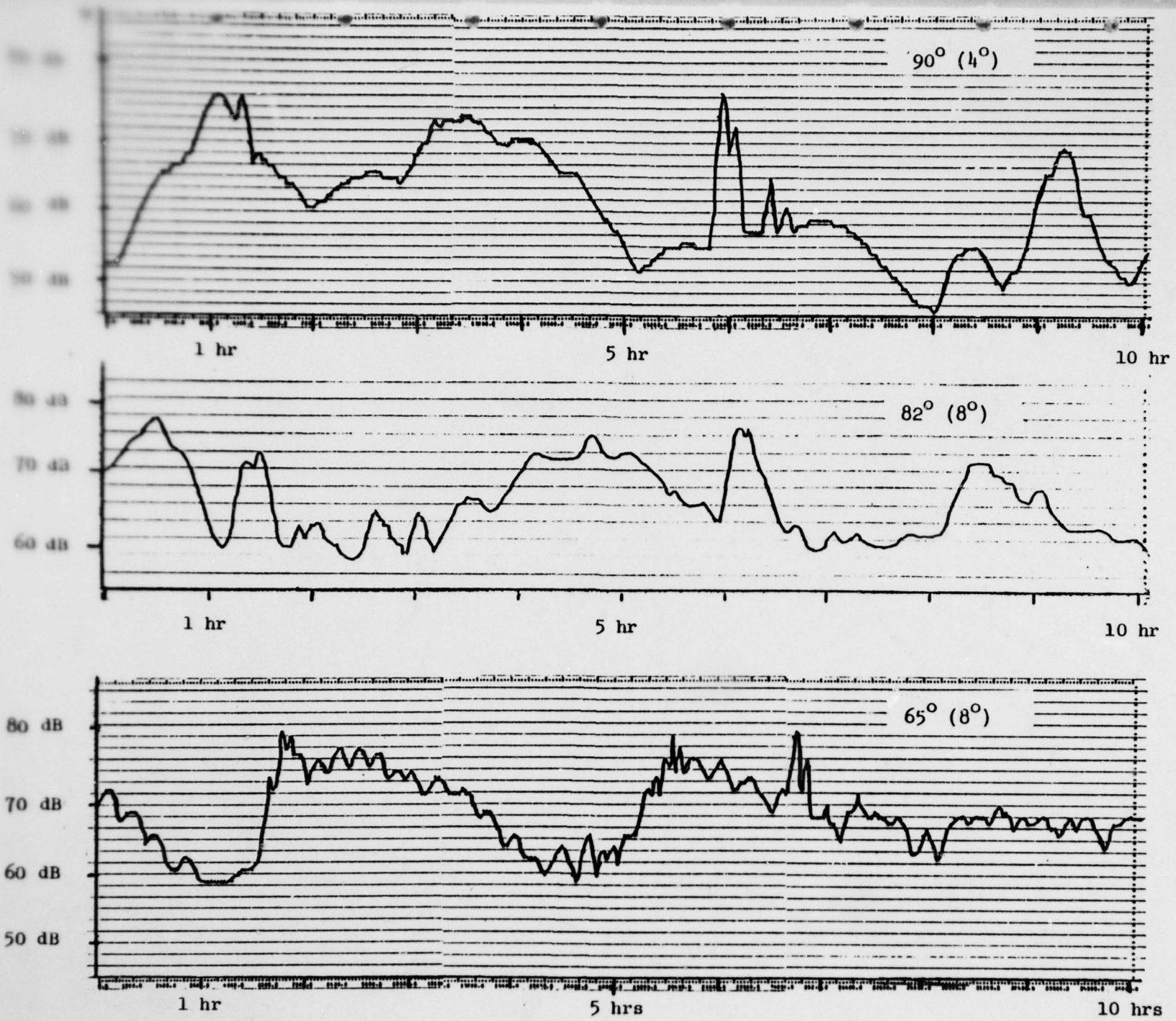

Figure 6-3 Beam Noise Time Series (Case 2)

The plots show the effects of ships moving this way and that across the array. It is also instructive to compare with the omni noise of Figure 5-2.

In each of the sample series notice that the fluctuations are rather slow - i.e., the periods are long. Because the shipping lanes are nearly perpendicular to the beam axis, typical radial ship speeds are on the order of 0 to 5 knots. Since the important TL fluctuation periods are on the order of 1 nm or more, the fastest fluctuations should have periods of about ten or fifteen minutes. Likewise, the time for a ship to cross the beam is on the order of one hour at 100 nm and five hours at 500 nm. These figures are consistent with the pictures. Also notice that as the steering angle decreases, the low amplitude fluctuations become more rapid, showing that the TL fluctuations become more important as noise sources cross the beam with greater radial speeds.

6.1.2 Sidelobe Contributions

The effect of sidelobe suppression is typified by Figure 6-4 and the upper plot of Figure 6-3. Here noise from the broadside beam with 4^{o} beamwidth and 30 dB sidelobe suppression is compared with that for infinite suppression. From the discussions of Appendix G, the greatest sensitivity is expected at narrow beamwidths. Even in this case, the differences are apparent only at the lowest levels of noise. Statistics of the fluctuations, including the autocovariance, for fifty replications showed that there is no appreciable difference between the 30 dB and infinite-suppression time series of beam noise.

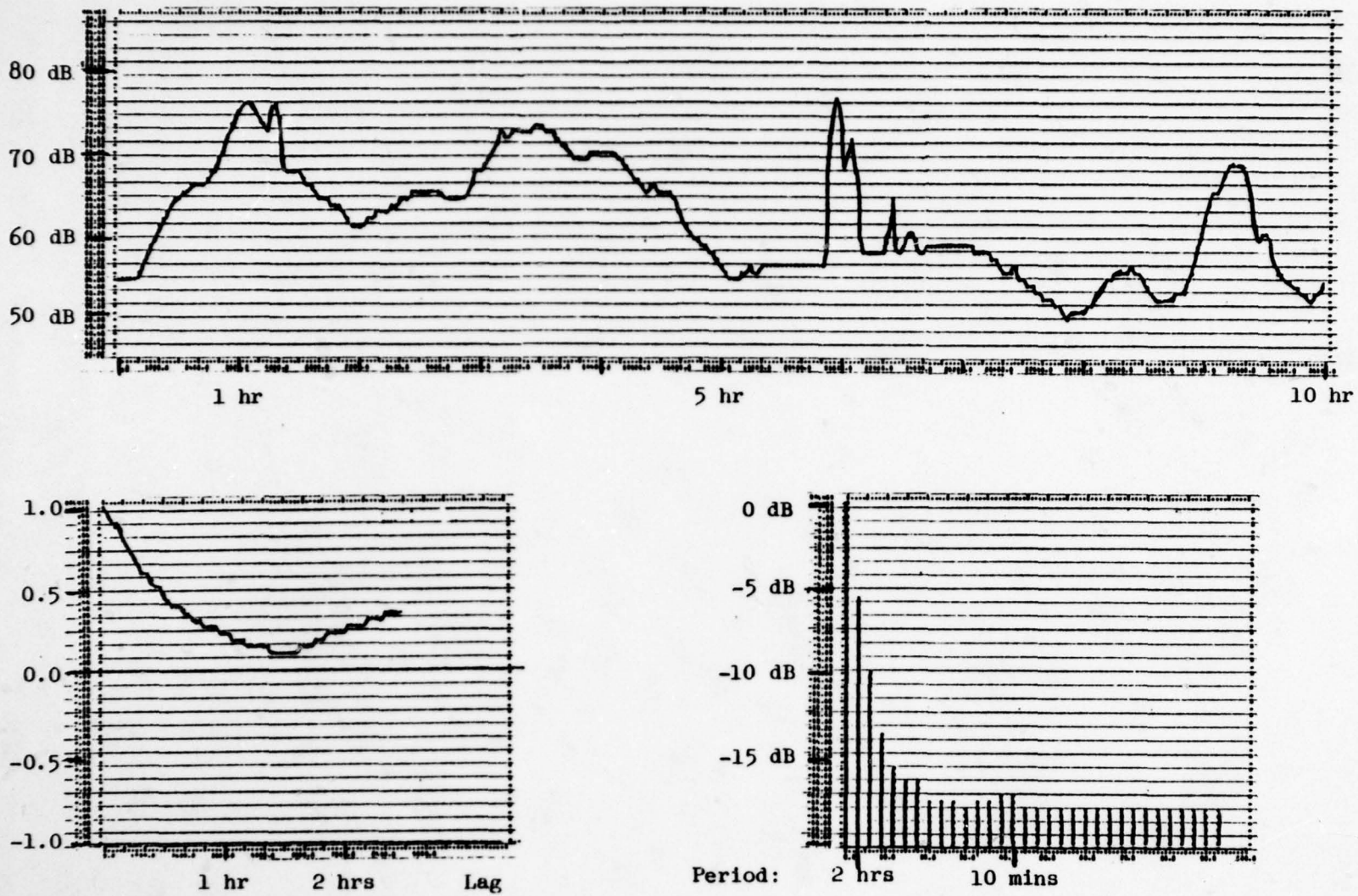

Time Series, Autocovariance and Spectrum for Beam Noise (#2)
90^{o} Beam, 4^{o} Beamwidth, 30 dB Sidelobe Suppression

Figure 6-4

6.1.3 Moments and Distributions

Table 6-1 shows percentiles for the sample mean, standard deviation, skewness, and kurtosis derived from the fifty ten-hour noise time series and various beams and beamwidths. Since there is probably an undersampling problem (there may be as few as ten uncorrelated samples in a ten hour series), the ensemble statistics over the fifty replications have also been calculated at 15 time points; the results are displayed in Table 6-2.

The first thing to notice is that the ensemble and time estimates of mean and variance are nearly identical, supporting the assumption of ergodicity. Other significant properties of these data include:

(i) The mean levels decrease by about 4 dB as the beamwidth decreases from 8° to 4°. At the same time, the variance increases by at least 1 dB and the skewness tends to decrease.

(ii) The levels increase by about 1.5 dB from the 90° to the 65° beam (8° beamwidth), although the variance and skewness seem to be invariant.

(iii) Refer to the omni noise data (Section 5), and note that the 8° beamwidth levels are down about 17 dB from the mean omni

Beam (Width)	Sidelobe Suppression	Mean	Standard Deviation	Skewness	Kurtosis
90° (8°)	30 dB	65.8 dB 67.0 68.5	3.4 dB* 4.1 5.0	0.1 0.7 1.6	-0.7 1.0 4.8
82° (8°)	30 dB	66.0 dB 67.0 67.8	2.7 dB 3.2 4.7	0.1 0.7 1.4	-0.9 0.4 4.4
65° (9°)	30 dB	67.5 dB 68.4 69.5	2.8 dB 3.8 4.5	0.1 0.7 1.8	0.0 1.1 6.1
90° (8°)	∞	65.6 dB 66.9 68.5	3.3 dB 4.0 4.8	0.0 0.5 1.5	-0.6 1.0 4.5
90° (4°)	30 dB	61.0 dB 62.6 64.3	4.7 dB 5.3 6.2	-0.1 0.2 0.8	-0.7 0.2 2.0
90° (8°) 35 Hour Sample	30 dB	66.2 dB	4.3	0.9	---

*The three numbers in each box are the 20th, 50th, and 80th percentiles for 50 ten-hour replications.

Time-Sampled Statistics of Beam Noise

Table 6-1

Beam (Width)	Sidelobe Suppression	Mean	Standard Deviation	Skewness	Kurtosis
		65.7 dB*	3.8 dB	-0.2	-0.7
90°	30 dB	66.7	4.3	0.0	0.1
(8°)		67.8	4.7	0.4	0.7
		65.3 dB	2.4	-0.3	-1.7
82°	30 dB	66.0	2.8	0.1	-1.2
(8°)		68.3	4.5	0.7	-0.5
		67.8 dB	3.4	-0.1	0.0
65°	30 dB	68.4	3.9	0.6	0.5
(9°)		69.0	4.4	1.1	2.1
		65.5 dB	3.9 dB	-0.4	-0.6
90°	∞	66.3	4.5	0.0	0.1
(8°)		67.5	4.8	0.4	0.6
		61.6 dB	5.4 dB	-0.3	-0.9
90°	30 dB	62.9	5.7	0.0	-0.4
(4°)		63.6	6.2	0.3	0.8

*20^{th}, 50^{th}, and 80^{th} percentiles over 50 ten-hour replications.

Ensemble Statistics of Beam Noise
(15 Time Points Over 50 Replications)
Table 6-2

levels, while the standard deviation for the 8° beamwidth is twice that for the omni case. The skewness of the omni data is significant and positive (1-3) while that for the beam data is typically near zero or negative.

(iv) The moments for the 35-hour sample are consistent with the other statistics.

The only point which requires further discussion is the change in levels from omni to 8°-beam noise to 4°-beam noise. Since the expected number of ships contributing in each case decreases from 155 to 8 to 4, the mean intensity is expected to decrease by about 13 dB and 3 dB instead of the 17 dB and 4 dB observed. This discrepancy is ascribed to the fact that the means derived from the time series are averages of dB-variables, which have different skewness according to the number of ships contributing. The 4 dB and 1 dB differences result from the displacement of the mean of the log from the log of the mean. Similarly, the increase by 1.5 dB in mean level from the broadside (90°) beam to the 65° beam is attributed to an increase in the expected number of ships (from eight to nine) and the change in the distribution of ships present.

Sample distribution functions for beam noise were constructed from the time-series data but were typically undersampled. As the small positive and negative skewness of the beam noise would suggest, the sample

(intensity) distributions were most often accepted by the Kolmogorov test as log-normal or chi-square (2 d.f. and higher) at the 5% level.

6.1.4 Correlation Properties

The autocovariance functions for beam noise shown in Figures 6-1, 6-2 and 6-4 are representative examples of the 50 replications. They are adequately fitted by decaying exponentials.

Table 6-3 gives the percentiles of decorrelation times for the various beams as derived from the 50 replications. The most concrete conclusion to be made is that both beam noise and omni noise have decorrelation times of 0.5 to 1.0 hour and zero-crossings at 1.5 to 2.5 hours. The fluctuation time scales for ships on the beam (periods of at least 10 or 15 minutes driven by TL) and the long waiting periods for ships to arrive on a beam (.8 hours) are consistent with these figures.

The spectra of Figures 6-1, 6-2, and 6-4 reinforce the argument that the long-term trends (periods of one hour or more) can dominate the temporal properties of both beam noise and omni noise. On the other hand, when a few noise sources have significant radial velocity components, the faster (TL-induced) fluctuations also become important - as noted in the case of the 65° beam. Appendix G gives rules of thumb for determining the relative importance of beam-pattern and TL fluctuations for a single moving source.

Beam (Width)	Decorrelation Time (minutes)			Time to First Zero-Crossing of Autocovariance Function (minute)		
	20th Percentile	Median	80th Percentile	20th Percentile	Median	80th Percentile
90° (8°)	20	64	72	76	92	150+
90° (4°)	24	42	57	40	87	150+
65° (8°)	30	34	70	50	67	150+
90° (8°) 35-Hour Sample		28			138	
Omni	20	25	60	40	95	130
Omni 35-Hour Sample		56			156	

Beam-Noise Decorrelation Times
(50 Replications of Ten-Hour Duration)
Table 6-3

6.1.5 Level-Crossing Properties

Although noise replications were generated for nine array beams, the level-crossing properties are calculated only for the broadside beam with 8^{o} beamwidth and 30 dB sidelobe suppression. The statistics are summarized in Table 6-4 (the first number in each triplet) for threshold levels equal to the mean, $\mu = 67.1$ dB, and to $\mu \pm \sigma$. They were derived from many ten-hour realizations of the DSBN model and represent average values. The spreads about them were wide in all categories. The nearly symmetric and Gaussian nature of the data is reflected in the values P(N>L) and P(N<L). The cumulative probabilities and waiting times are consistent with the average decorrelation time of 36 minutes.

Finally, for the distribution of interval lengths with N>L or N<L, the case N<L is focussed upon here. Two samples from the fifty replications of beam noise were selected as representative of the diversity in the distribution of lengths. They might be viewed as 20th and 80th percentile curves, since they were chosen with that in mind, although no objective criteria were applied. Table 6-5 shows counts of interval lengths for three threshold levels ($L = \mu, \mu+\sigma, \mu-\sigma$) and the two samples under the labels Acoustic Simulation #1, #2. The values are representative of data which consistently show up to two short intervals (<10 minutes), one or two intermediate-length intervals (10-60 minutes), and, according to L, zero to three long intervals (60-200 minutes) in a 600 minute sample. A single long interval at the lowest threshold level occurs when the beam sees only a few distant

Sample Statistics	L = μ−σ = 63.4 dB			L = μ = 67.1 dB			L = μ+σ = 70.8 dB		
P(N>L)	.85	.84	.84	.54	.50	.50	.15	.16	.16
Expected Wait for N>L (mins)	7.0	6.8	4.6	23.7	36	31	66	190	170
P(N>L) at least once in 60 min interval	.95	.96	.91	.82	.78	.70	.52	.36	.37
P(N<L)	.15	.16	.16	.46	.50	.50	.85	.84	.84
Expected Wait for N<L (mins)	210	190	168	41	36	31	4	6.8	4.6

First number is average over acoustic simulations ($\mu = 67.1$, $\sigma = 3.7$, $\tau = 36$ mins).

Second number is expected value for Jump process with same (μ, σ, τ).

Third number is median of GM-process replications with same (μ, σ, τ).

Level-Crossing Statistics for Beam-Noise Time Series
(90^{o} Beam, 8^{o} Beam Width)
Table 6-4

		Interval Length k (minutes)				
	Simulation	2 -10	10 -30	30 -60	60 -100	>100
L = μ-σ	Acoustic #1	1	2	0	0	0
	Acoustic #2	0	1	1	0	1
	GM #1	1	2	0	0	0
	GM #2	6	2	2	0	0
	Jump #1	1	0	0	0	0
	Jump #2	2	0	0	0	1
L = μ	Acoustic #1	2	1	1	0	1
	Acoustic #2	2	1	1	1	1
	GM #1	6	8	1	0	0
	GM #2	9	4	1	0	0
	Jump #1	1	1	0	2	1
	Jump #2	2	3	1	1	1
L = μ-σ	Acoustic #1	0	1	1	0	3
	Acoustic #2	1	0	1	2	1
	GM #1	5	1	0	1	2
	GM #2	4	0	1	2	1
	Jump #1	0	0	0	0	2
	Jump #2	0	1	0	0	1

Number of Intervals of Length k with N<L

Level-Crossing Properties for
Representative Samples of Acoustic and Stochastic
Beam-Noise Time Series of Ten-Hour Duration

Table 6-5

ships or ships between convergence zones. The probability of such a situation enduring for an hour or more in a ten hour period is high for the 8° beamwidth and the given ship distribution.*

6.2 Properties of Stochastically Modeled Beam Noise

The moments, sample distributions, autocovariance, and spectra for the GM and Jump processes have all been discussed in Subsection 4.2. Although the GM process looks more like the beam-noise series, the Jump matches the above-mentioned properties just as well. In fact, the acoustic simulations show one-dimensional distributions which are nearly Gaussian and autocovariance functions which are approximately exponential.

As far as the level-crossing characteristics are concerned, Table 6-4 compares summary data for the random processes with those for the acoustic model discussed above (90° beam, 8° beamwidth, etc.). Except for the cumulative probabilities and the wait for N>L at $L = \mu + \sigma$, the two processes yield estimates which (on average) are in good agreement with the acoustic noise data. There is again an undersampling problem inherent in these numbers since there are in each ten-hour series an average of only about 20 "uncorrelated" time samples. Nonetheless, the aggregated results suggest that the random process models are reasonable candidates for simulating beam-noise data.

*For example, the chance of having eight or fewer ships on the main beam (and its image) and all beyond 200 nm is more than 0.1.

For a final measure, compare the distribution of interval lengths (with N<L) for sample paths of the random-process model with the acoustic data in Table 6-5. Just as for the acoustic simulation distributions, the values labled "GM #1," "#2," and "Jump #1," "#2" were derived from representative, but diverse samples paths of the GM and Jump processes. They can also be compared with the entries of Table 4-7 for the A+BlogR average $\overline{TL}$, which are calculated on a different scale but again representative. Comparison of values for these samples suggests the conclusions that:

- As noted in the simulation of TL, the GM process tends to predict too many short intervals and too few long ones.

- The Jump process is in reasonably good agreement with the acoustic data for all values of L.

6.3 Summary

For the test cases considered here, the Jump and GM random-process models can adequately simulate the acoustic beam-noise data, provided that accurate inputs (μ,σ,τ) are used. This conclusion is similar to that for the transmission-loss data; however, the estimation of input parameters may be even more difficult.

As noted in 6.1.3, the mean, variance, and shape (e.g., skewness) of the beam-noise distributions

AD-A055 675 SCIENCE APPLICATIONS INC MCLEAN VA F/G 17/1
ACOUSTIC FLUCTUATION MODELING AND SYSTEM PERFORMANCE ESTIMATION--ETC(U)
JAN 78 R C CAVANAGH N00014-76-C-0753
UNCLASSIFIED SAT-79-737-WA-VOL-1 NL

2 OF 2
ADA
055675

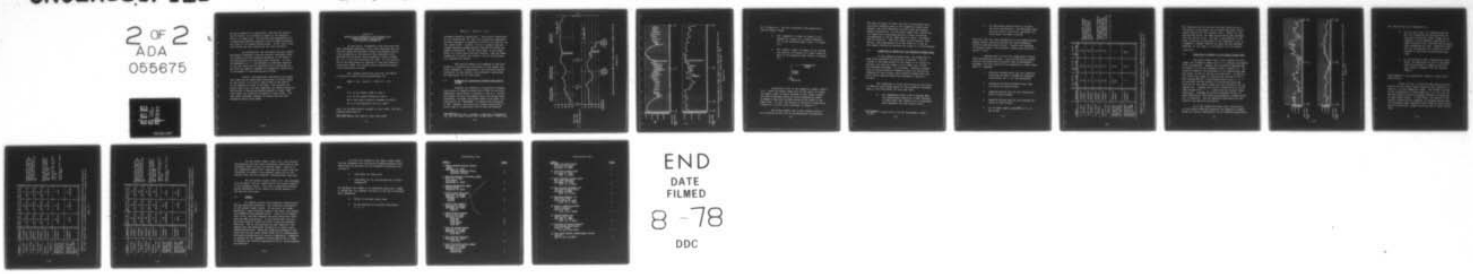

END
DATE
FILMED
8-78
DDC

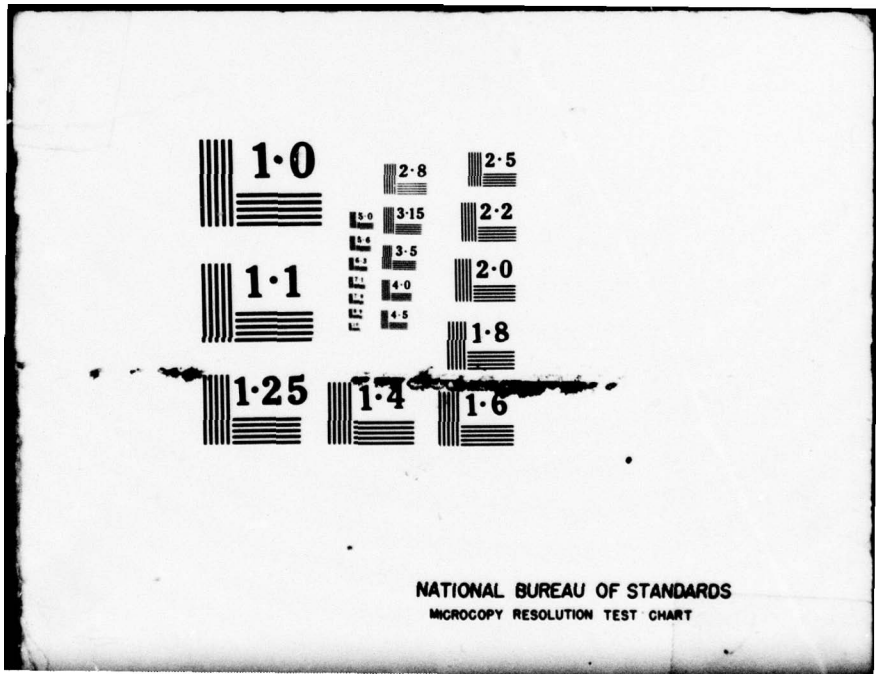
1·0
1·1
1·25
1·4
1·6
1·8
2·0
2·2
2·5
2·8
3·15
3·5
4·0
4·5
NATIONAL BUREAU OF STANDARDS
MICROCOPY RESOLUTION TEST CHART

are quite sensitive to beam width; they and the decorrelation time do not necessarily depend on the shipping field in a simple way. Calculating these parameters with a large-scale computer simulation such as DSBN eliminates the value of the random-process model - since "real" noise time series and their properties are then available.

As alternatives, the chi-square and shot models mentioned in Appendix D provide analytic techniques which can potentially yield adequate estimates of the shape of the distribution and autocovariance functions. In fact, the dependence of μ,σ and skewness on beamwidth observed in the test cases can be explained with a chi-square model when the number of degrees of freedom are proportional to the number of contributing ship sources.

Finally, the beam-noise time-series plots show that there can be significant excursions in levels caused by the arrival of a loud or nearby ship on the beam or by the absence of ships on the beam. The narrower the array's main lobe, the more important are these occurrences. The details of system performance depend on these "beam free times" and durations of higher or lower noise. The shot model provides a method for simulating such ship movements across array beams.

Section 7

RESULTS FOR ACOUSTICALLY AND STOCHASTICALLY MODELED SIGNAL-TO-NOISE RATIO AND DETECTION PROPERTIES

To this point, transmission loss and noise have been considered separately, and it was concluded that for the test cases the stochastic models can simulate statistical properties of the acoustic data reasonably well, provided that accurate input parameters (2-mile average TL; (μ,σ,τ) for ΔTL and noise) are used. In this section, the TL and beam noise are combined to form the signal-to-noise ratio (SNR), the variable which determines whether or not detections are made.

For a stable source with level SL, the SNR as a function of time is given approximately by*

$$SNR(t) = SL - TL(R(t)) + BP(\phi(t)) - N(t)$$

where

$R(t)$ is the target range at time t,

$\phi(t)$ is the target bearing at time t,

BP is the array intensity response (in dB's),

$N(t)$ is the beam-noise level at time t.

Thus, for the SNR detector assumed in this study, the level-crossing properties of

*For ship speeds much smaller than sound speed

$$BP(\phi(t)) - TL(R(t)) - N(t)$$

determine detection properties.* The relative importance of the variables BP, TL, and N as fluctuation components has been discussed in Appendix G and will be noted for the test cases below. Clearly, if R(t) is nearly constant (target distance changes slowly) then BP will drive the signal fluctuations. On the other hand, if the target moves on a radial path from the receiver, then the range change will be rapid, BP constant, and TL fluctuations will dominate for signal.

This section begins with examples of SNR time series to illustrate the interaction of the signal and noise components. Comparisons of the detection-related statistics for the acoustic and stochastic simulations are then given for the test cases.

7.1 Examples of Acoustically Modeled Time Series of SNR

Consider the examples of acoustically modeled time series of signal-to-noise ratio (SNR) at the array beamformer output shown in Figures 7-1 and 7-2. Without the benefit of prior information about the TL and noise properties, one might note some trends in the data, but rely heavily on "randomness" to explain the variations in SNR. However, the plots use a single replication of noise (Case #1 of Sections 5 and 6) and the detailed

*The SNR detector has a constant recognition differential R_D, and the signal excess (SE) is then $SE(t) = SNR(t) - R_D$.

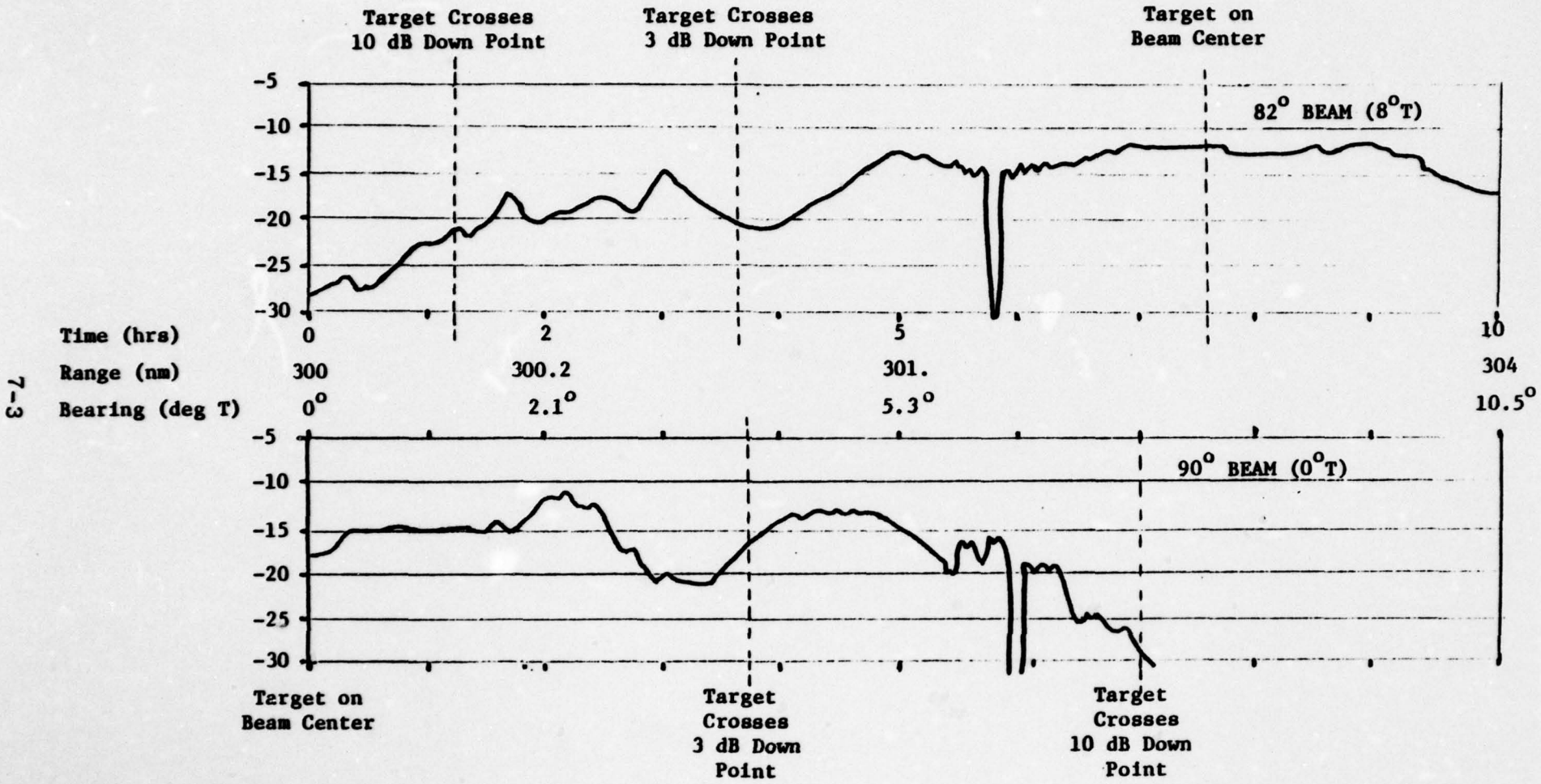

Acoustically Simulated SNR for 5-knot Tangential Target at 300 nm

Figure 7-1

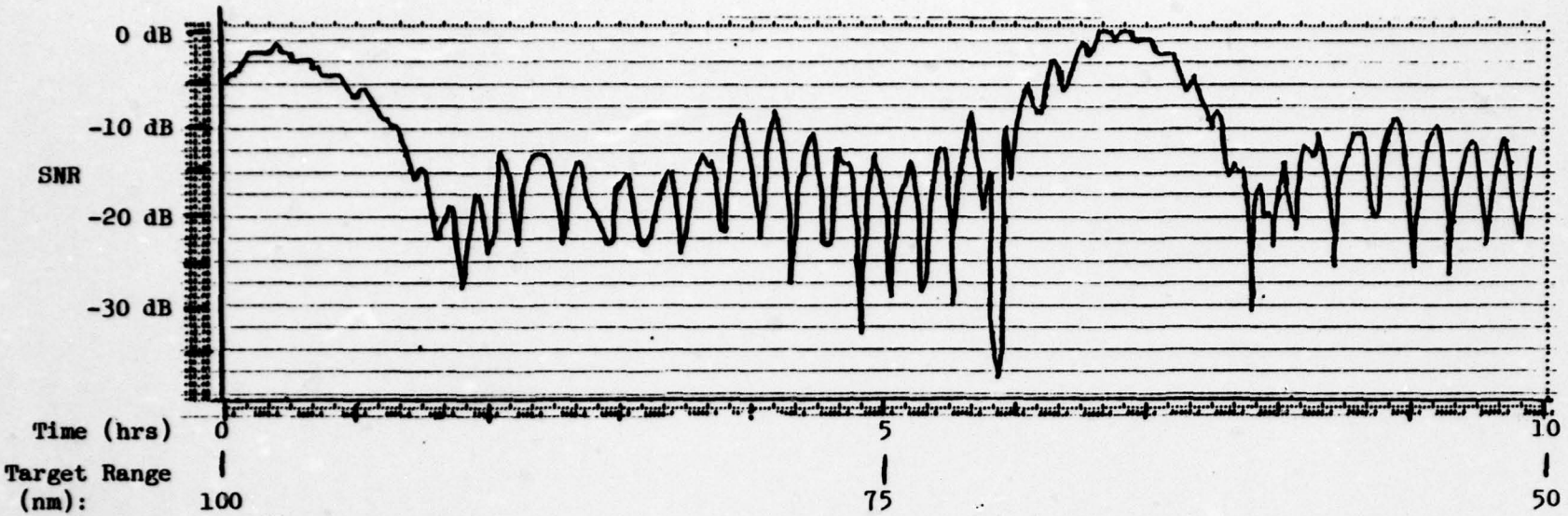

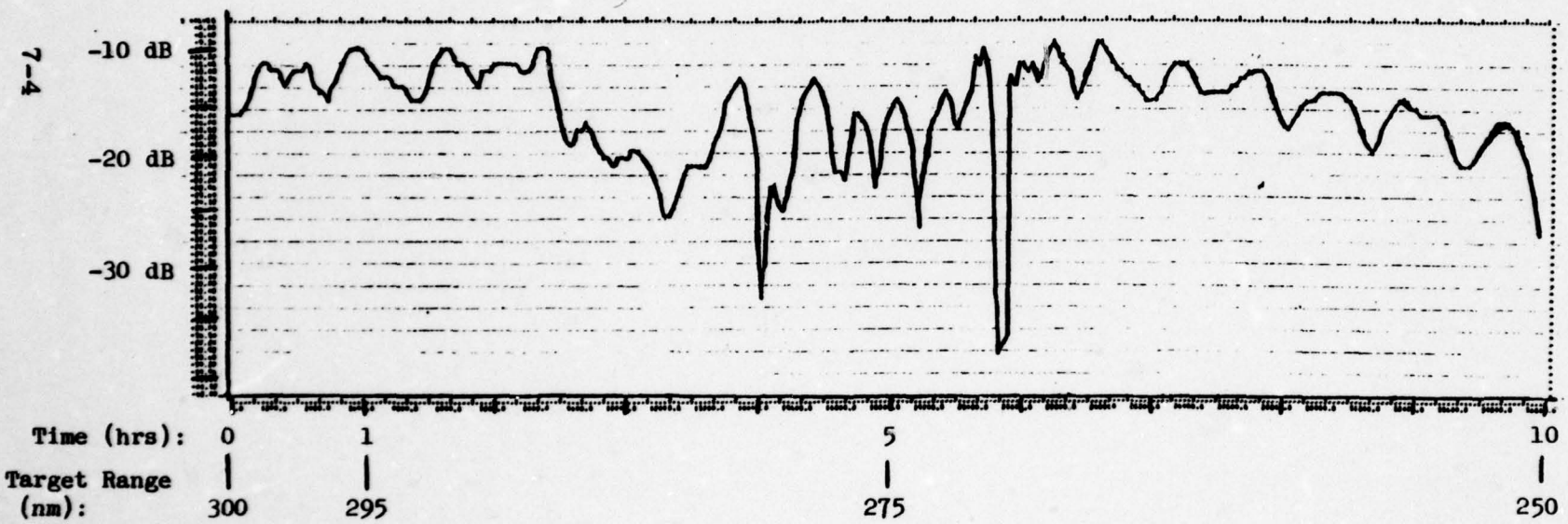

Acoustically Simulated SNR for Radial Target at 5 Knots and 155 dB Source Level
Array Steering = 90^{O} (0^{O}T), Target Bearing = 0^{O}T

Figure 7-2

TL of Figure 4-1. The only difference then among plots are the target tracks:

- The "tangential" target in Figure 7-1 is opening at 5 knots on a course perpendicular to the broadside beam (Track 1 of Figure 2-1)

- The "radial" target in Figure 7-2 is closing the receiver at 5 knots on a track along the axis of the broadside beam (Track 3 of Figure 2-1).

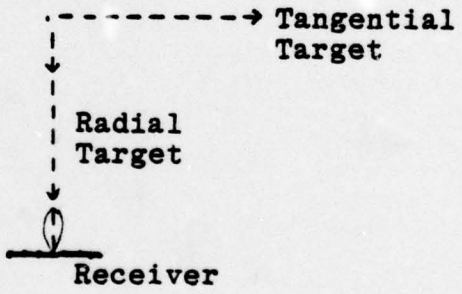

Concentrate first on the tangential target (Figure 7-1). Since the radial range rate is only about 0.7 knots, the signal level is nearly constant as the target crosses the beam (3 dB-down points for array response are shown as dashed lines) and the SNR variations are those of the beam noise. In fact, the details of the plot of beam noise (Figure 6-1) can be found (inverted) in Figure 7-1.

The radial-target case is more complex since it is influenced by both the TL and beam-noise fluctuations.

The data of Figure 7-2 show the slow but pronounced noise variations observed above in the tangential-target case. However, the noise modulates the more rapid and regular signal fluctuations. For the short range case (100-50 nm), the signal has a pronounced period of about 10 minutes, corresponding to the TL range period of about 1 nm identified in Section 4. When the target is more distant (300-350 nm), the range period is on the order of 1.5 nm, so that signal fluctuation periods are closer to 15 or 20 minutes.

7.2 Comparison of Models for the Tangential-Target Case

In the tangential-target case, the properties of beam noise determine the detection properties. The influence of the beam pattern on the signal is of course important, but once the target is on a beam (e.g., within the 3-dB-down bearings), it is minimal. Detection properties at various detector threshold levels can thus be determined for both acoustic and stochastic models from the noise level-crossing properties discussed in Section 6 for N<L*.

The comparison of fifty replications of the acoustic SNR with many sample paths for the stochastic processes leads to the conclusions for this case that:

- For thresholds within 4 dB of the mean SNR, the Jump-process simulation of SNR (actually, of beam noise) was judged to be in reasonably good agreement with the acoustic data.

*To convert, a noise level of 67 dB corresponds to SNR = -15 dB.

- The GM-process results were not as good, but still satisfactory. The Ehrenfest model was also used in this test, and showed results about the same as the GM.

Note well that the input parameters for the random-process models (noise statistics and mean TL) were determined directly from the acoustic data. Without the advantage of accurate inputs, the stochastic simulations can be expected to fail.

Consider next a few of the comparisons on which these conclusions are based. Since the detection parameters are the quantities ultimately used in performance analyses, the test statistics are presented in those terms. Table 7-1 compares:

- detection probabilities (P_D) for detectors requiring the SNR to exceed the threshold continuously for 2, 10, and 30 minutes
- cumulative detection probabilities (CP_D) for 60-minute opportunities
- expected waiting time for the 2-minute detector to gain contact
- expected waiting time for the 2-minute detector to lose contact
- all for mean signal excess($\overline{SE}$) of -4, 0, and +4 dB.

Property	Simulation	$R_D \simeq -11$ dB ($\overline{SE} \simeq -4$ dB)	$R_D \simeq -15$ dB ($\overline{SE} \simeq 0$ dB)	$R_D \simeq -19$ dB ($\overline{SE} \simeq +4$ dB)
P_D for 2-min. Detector	Stochastic	.16	.50	.84
	Acoustic	.15	.46	.83
P_D for 10-min. Dectector	Stochastic	.13	.43	.83
	Acoustic	.13	.42	.76
P_D for 30-min. Detector	Stochastic	.12	.30	.71
	Acoustic	.12	.35	.64
60-minute CP_D for 2-min. Detector	Stochastic	.36	.78	.95
	Acoustic	.28	.72	.93
Expected Waiting Time for Detection by 2-min. detector (minutes)	Stochastic	190	35	7
	Acoustic	210	40	4
Expected Waiting Time for Loss of Contact by 2-min. Detector (minutes)	Stochastic	7	35	190
	Acoustic	7	25	65

*Values labeled "Acoustic Simulation" are derived from averages over 50 ten-hour replications of the acoustic noise model.

*Values labeled "Stochastic Simulation" are averages over many sample paths for the Gauss-Jump model of noise using the acoustically-derived parameters:

$(\mu, \sigma, \tau) = (67.1, 3.7, 36)$.

Comparison of Acoustically and Stochastically Modeled Detection Properties* for Tangential Target on Broadside Beam of 8^o Width and at Range 300 nm

Table 7-1

The table entries are derived from many replications of the acoustic noise model and the Gauss-Jump model (using inputs derived from the acoustic data). Except for one waiting-time entry, the Jump process shows good agreement with the acoustic data. The small discrepancies in the other values can be explained by the Jump-model's use of a symmetric (normal) density for noise and the observed skewness (to the right) of the density for the acoustic noise data.

7.3 Comparison of Models for the Radial-Target Case

The radial-target case is more complex and challenges the stochastic models since it is strongly influenced by TL fluctuations. Compare the acoustically modeled SNR of Figure 7-2 with the stochastic data in Figure 7-3. The latter is based on the difference of two Jump-process sample paths, one for TL and one for beam noise. In particular, the TL for signal is simulated as the sum of the 2-mile average $\overline{TL}$ and a Jump process whose inputs (μ, σ, τ) are derived from the acoustic TL fluctuation data over 2-150 nm for the nearby target and over 100-500 nm for the distant one. Likewise the noise is simulated as a second Jump process with (μ, σ, τ) taken from the acoustic beam-noise data. Although the plots of Figures 7-2 and 7-3 show similarities, the nulls and periods are indeed different in character. But the important properties are measured by the detection statistics.

As in the tangential-target case, replications of the acoustic SNR were generated and compared to sample paths for various combinations of the random-process models.

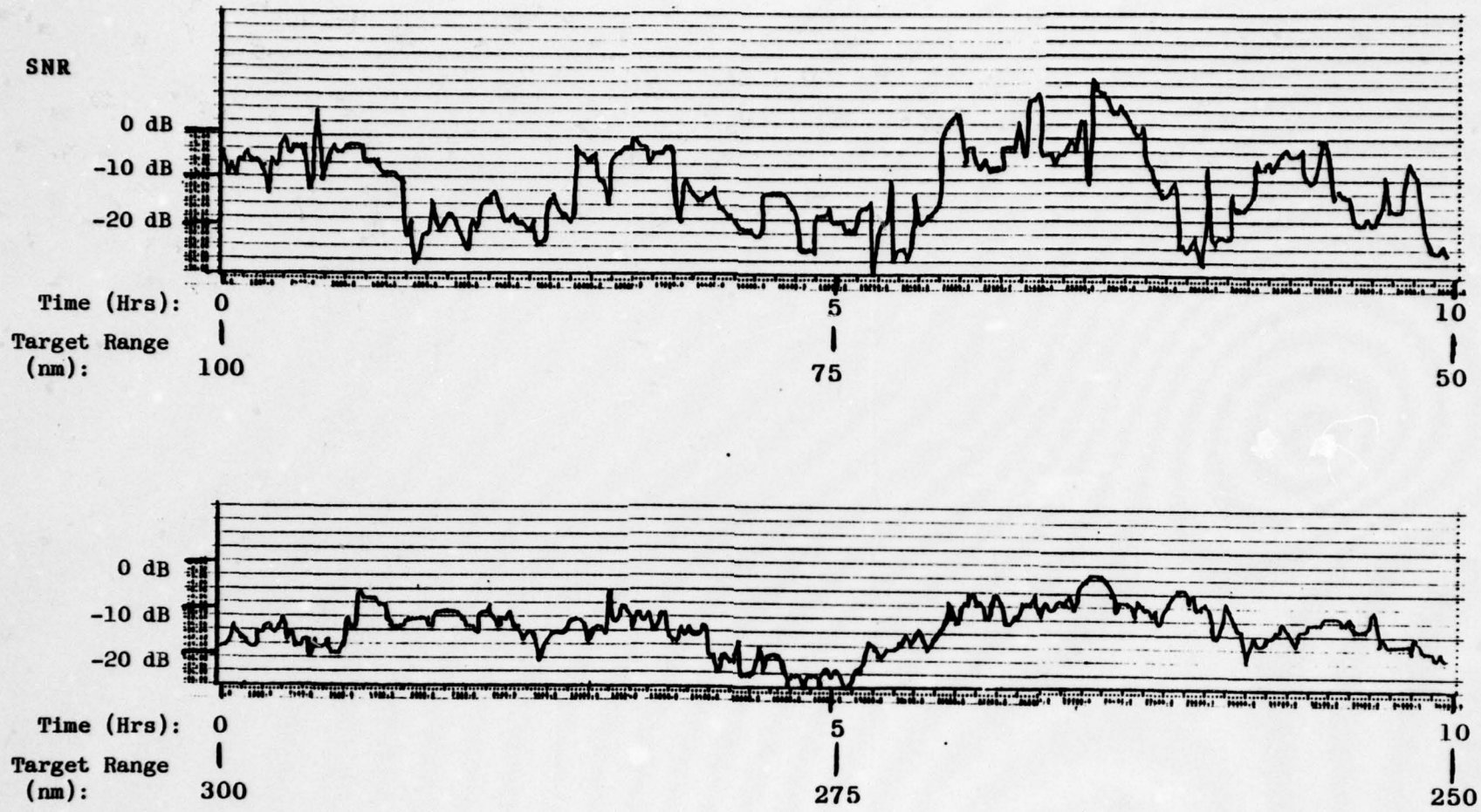

Stochastically Simulated SNR for Radial Target at 5 Knots and 155 dB Source Level

Figure 7-3

The conclusions can be summarized as:

- For the test cases, the random-process models for simulating TL and beam noise for both near and distant radial target can be combined to yield adequate simulations of signal-to-noise ratio, provided that accurate input parameters are used. Especially important is the smoothed TL (a 5-mile or finer average is indicated) and mean beam-noise level.

- Of the stochastic model combinations considered, the Jump model for both TL and beam-noise fluctuations is judged to give the best overall agreement with the acoustic results.

Some examples of the comparisons leading to these conclusions follow.

Tables 7-2 and 7-3 show the same statistical properties for the radial target tracks as were displayed in Table 7-1 for the tangential target. The values of recognition differential in these cases (R_D = -6, -12, and -18 dB) were chosen to give a reasonable spread of conditions of mean signal excess. In each table, the results of the acoustic simulation are compared to averages derived from the stochastic model described above (Jump for both TL and noise fluctuations), judged to be the best of those considered.

Property	Simulation	$R_D \simeq -6$ dB	$R_D \simeq -12$ dB	$R_D \simeq -18$ dB
P_D for 2-min. Detector	Stochastic	.27	.46	.71
	Acoustic	.21/.26/.31	.41/.46/.50	.69/.71/.77
P_D for 10-min. Detector	Stochastic	.14	.29	.53
	Acoustic	.13/.15/.23	.27/.28/.32	.41/.49/.50
P_D for 30-min. Detector	Stochastic	.04	.16	.30
	Acoustic	.06/.09/.16	.16/.19/.23	.25/.31/.35
60-minute CP_D for 2-min. Detector	Stochastic	.63	.90	1.0
	Acoustic	.42/.50/.55	.72/.80/.83	.97/.99/1.0
Expected Waiting Time for Detection by 2-min. Detector (minutes)	Stochastic	49	15	4
	Acoustic	76/84/100	20/27/40	2/4/7
Expected Waiting Time for Loss of Contact by 2-min. Detector (minutes)	Stochastic	5	12	25
	Acoustic	4/5/11	12/14/18	21/25/28

*Values labeled "Acoustic Simulation" are 20th, 50th, 80th percentiles over 10 ten-hour replications of the acoustic noise and signal.

*Values labeled "Stochastic Simulation" are averages over many sample paths of SNR, using the:

-Gauss-Jump model for noise with $(\mu, \sigma, \tau) = (67.1, 3.7, 36)$

-Gauss-Jump + 2-mile average TL for signal

Comparison of Acoustically and Stochastically Modeled Detection Properties* for 5-knot Radial Target on Broadside Beam of Width 8^{o}, at Ranges 100-50 nm

Table 7-2

Property	Simulation	$R_D \simeq -6$ dB	$R_D \simeq -12$ dB	$R_D \simeq -18$ dB
P_D for 2-min. Detector	Stochastic	.04	.28	.70
	Acoustic	.00/.05/.12	.21/.32/.48	.70/.75/.84
P_D for 10-min. Detector	Stochastic	.00	.19	.58
	Acoustic	.00/.02/.04	.11/.22/.44	.58/.65/.71
P_D for 30-min. Detector	Stochastic	.00	.11	.44
	Acoustic	.00/.00/.00	.00/.20/.29	.39/.53/.55
60-minute CP_D for 2-min. Detector	Stochastic	.26	.58	.96
	Acoustic	.00/.17/.35	.48/.65/.72	.87/.97/1.0
Expected Waiting Time for Detection by 2-min. detector (minutes)	Stochastic	130	60	7
	Acoustic	132/206/600	38/46/98	2/6/15
Expected Waiting Time for Loss of Contact by 2-min. Detector (minutes)	Stochastic	0	7	46
	Acoustic	0/0/2	3/10/24	40/48/70

*Values labeled "Acoustic Simulation" are 20th, 50th, 80th percentiles over 10 ten-hour replications of the acoustic noise and signal.

*Values labeled "Stochastic Simulation" are averages over many sample paths of SNR, using the:

-Gauss-Jump model for noise with $(\mu, \sigma, \tau) = (67.1, 3.7, 36)$

-Gauss-Jump + 2-mile average TL for signal

Comparison of Acoustically and Stochastically Modeled Detection Properties*
For 5-knot Radial Target on Broadside Beam of Width 8^{o}, at Range 300-250 nm

Table 7-3

For the nearer target (Table 7-2), the principal discrepancies are the overly optimistic predictions by the stochastic model of P_D's and Waiting Times. Just as in the tangential-target case, these may well result from the difference in shapes of the marginal densities for the acoustic data and the (Gaussian) random-process densities.

For the distant target (Table 7-3), the discrepancies are small, and not clearly due to any single property of the stochastic model. The lack of complicated bottom-bounce propagation is one reason for better behavior of the data for this case.

7.4 Summary

To compare acoustic and stochastic simulations of SNR and detection properties, this study has concentrated on two special target tracks. In one case, the target maintains a nearly constant range to the array, and crosses the broadside beam perpendicularly. Since the TL changes very little, the beam response and noise properties determine the SNR fluctuations. In the second case, the target moves radially toward the array, along the broadside beam axis. The TL fluctuations are then important, and combine with the beam-noise variability to yield a more complicated picture. These two cases are bounding in the sense that for any other target track the TL, beam-pattern, and noise fluctuations will occur in combination, somewhere in between the two (Appendix G offers some rules of thumb to estimate the relative importance of TL and array-response fluctuations).

For both the tangential and radial target cases, the best agreement with acoustically modeled detection probabilities was obtained for the stochastic simulation consisting of

- Jump model for beam noise
- Jump model for TL fluctuations and a 2-mile averaged $\overline{TL}$

The agreement was judged to be reasonably good over a range of thresholds, but depends critically on the use of accurate input parameters:

- Smooth TL and mean noise level
- TL and beam-noise fluctuation statistics (μ, σ, τ).

Distribution List

Address	Copies
1. Defense Advanced Research Projects Agency Washington, DC 20301	
(Tactical Technology Office)	1
(Technical Library)	1
2. Assistant Secretary of the Navy (R,E&S) ATTN: Dr. D. Hyde The Pentagon Washington, DC 20350	1
3. Defense Documentation Center Cameron Station Alexandria, VA 22314	2
4. Chief of Naval Operations Department of the Navy Washington, DC 20350	
(OP-987)	1
(OP-955)	1
5. Chief of Naval Material Department of the Navy Washington, DC 20360	
(ASW-13)	1
6. Office of Naval Research 800 N. Quincy Street Arlington, VA 22217	
(Code 431)	2
(Code 222)	1
(Code 102-OS)	1
(Code 486)	1
7. Naval Sea Systems Command Department of the Navy Washington, DC 20360	
(Code 06H2)	1
8. Naval Research Laboratory Washington, DC 20375	
(Code 8100)	2
9. Naval Electronics Systems Command Department of the Navy Washington, DC 20360	
(PME-124-62)	1
(NAVELEX 320)	1

Distribution List

Address	Copies
10. Center for Naval Analysis 1401 Wilson Boulevard Arlington, VA 22209	1
11. Naval Ocean Systems Center San Diego, CA 92152 ATTN: H. Schenk	1
12. Naval Underwater Systems Center New London Laboratory New London, CT 06329 ATTN: Mr. R. Hasse	1
13. Bolt, Beranek and Newman, Inc. 1701 North Fort Myer Drive Arlington, VA 22209 ATTN: Dr. M. Moll	1
14. Operations Research, Inc. 1400 Spring Street Silver Spring, MD 20910 ATTN: Dr. E. Moses	1
15. Daniel H. Wagner Associates Station Square One Paoli, PA 19301 ATTN: Dr. B. McCabe	1
16. Systems Control, Inc. 1801 Page Mill Road Palo Alto, CA 94304 ATTN: Dr. J. Anton	1
17. Institute for Acoustic Research 615 Southwest Second Avenue Miami, FL 33130 Mr. J.G. Clark (ATTN)	1
18. Naval Ocean Research andDevelopment Activity Code 320 Bay St. Louis, MS 39520	1